JACS
JOURNAL OF THE AMERICAN CHEMICAL SOCIETY

ARTICLE

pubs.acs.org/JACS

Hydrogenolysis of Palladium(II) Hydroxide, Phenoxide, and Alkoxide Complexes

Gregory R. Fulmer,[†] Alexandra N. Herndon,[†] Werner Kaminsky,[†] Richard A. Kemp,[*,‡,§] and Karen I. Goldberg[*,†]

[†]Department of Chemistry, University of Washington, Box 351700, Seattle, Washington 98195-1700, United States

[‡]Department of Chemistry and Chemical Biology, University of New Mexico, Albuquerque, New Mexico 87131, United States

[§]Advanced Materials Laboratory, Sandia National Laboratories, Albuquerque, New Mexico 87106, United States

Supporting Information

ABSTRACT: A series of pincer ($^{t\mathrm{Bu}}$PCP)Pd(II)−OR complexes ($^{t\mathrm{Bu}}$PCP = 2,6-bis($CH_2P^tBu_2$)C_6H_3, R = H, CH_3, C_6H_5, $CH_2C(CH_3)_3$, CH_2CH_2F, CH_2CHF_2, CH_2CF_3) were synthesized to explore the generality of hydrogenolysis reactions of palladium−oxygen bonds. Hydrogenolysis of the Pd hydroxide complex to generate the Pd hydride complex and water was shown to be inhibited by formation of a water-bridged, hydrogen-bonded Pd(II) hydroxide dimer. The Pd alkoxide and aryloxide complexes exhibited more diverse reactivity. Depending on the characteristics of the −OR ligand (steric bulk, electron-donating ability, and/or the presence of β-hydrogen atoms), hydrogenolysis was complicated by hydrolysis by adventitious water, a lack of reactivity with hydrogen, or a competing dissociative β-hydride abstraction reaction pathway. Full selectivity for hydrogenolysis was observed with the partially fluorinated Pd(II) 2-fluoroethoxide complex. The wide range of Pd−OR substrates examined helps to clarify the variety of reaction pathways available to late-transition-metal alkoxides as well as the conditions necessary to tune the reactivity to hydrogenolysis, hydrolysis, or dissociative β-hydride abstraction.

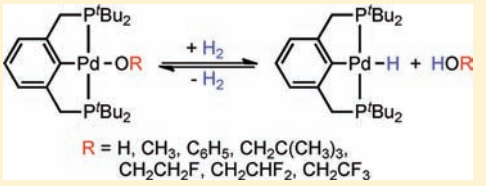

INTRODUCTION

Hydrogenation reactions play a very large role in homogeneous and heterogeneous metal catalysis, aiding in the production of a host of chemicals and pharmaceuticals.[1−3] A key reaction step in metal-catalyzed hydrogenation cycles is the formation of a metal hydride complex. This fundamental organometallic reaction has received extensive study, and as illustrated in Scheme 1, this hydride formation can proceed through a wide variety of mechanisms. Initial interaction of H_2 with the metal center typically proceeds via coordination and formation of an η^2-dihydrogen species.[4] Next, the reaction pathway could proceed via (**a**) oxidative addition (OA) to generate a metal dihydride species.[1,2] Notably, migratory insertion of a hydride to a bound olefin, followed by C−H reductive elimination of a hydrocarbon from this higher oxidation state species, would be a typical pathway for an olefin hydrogenation catalyst. An alternative reaction for the η^2-dihydrogen species would be (**b**) σ-bond metathesis (SBM), resulting in hydrogenolysis of the M−Y bond to generate a metal hydride complex along with the concurrent release of a hydrogenated ligand (H−Y).[5] Deprotonation of the dihydrogen moiety by (**c**) an external base or by (**d**) an internal base also results in formation of metal hydride species. The most prominent examples of pathway **d** are the well-known Noyori and Shvo-type catalytic systems for the hydrogenation of C═O and C═N bonds.[6,7] In these systems, the internal base is part of a chelating or multidentate ligand which prevents the dissociation of the protonated base.

Scheme 1

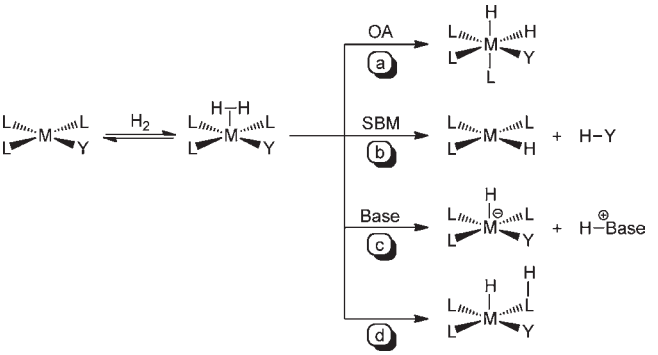

What happens if the heteroatom ligand (Y) receiving one of the hydrogens is a monodentate ligand such as a hydroxide, alkoxide, or amide group? While similar to SBM shown as path **b** in Scheme 1, reactions involving these ligand types would be mechanistically distinct since the lone pair on the ligand could be involved in the dihydrogen cleavage step, as in path **d**.[8,9] However, the reaction could also proceed via path **a** with H−Y reductive elimination from the dihydride species to yield the

Received: July 3, 2011
Published: September 21, 2011

same products. In fact, very little is known about this type of hydrogenation reaction, which results in hydrogenolysis of a metal−heteroatom bond. Contributing to the difficulty in studying this reaction for metal−hydroxide, −alkoxide, and −amide bonds are the variety of competing reactions available to metal complexes of these ligands. Hydrolysis and dissociative β-hydride abstraction (DBHA) are two relatively common competitive reactions noted for metal alkoxides and amides.[10,11] It is notable that DBHA leads to generation of the identical metal hydride formed in hydrogenolysis, albeit without production of the alcohol or amine. Instead, an unsaturated organic with a C=O or C=N bond is generated.

Despite the paucity of direct observation and mechanistic study of hydrogenolysis of late-transition-metal−oxygen bonds, the addition of hydrogen across M−OR bonds has been recognized to play a vital role in a number of important stoichiometric and catalytic reactions. For example, heterogeneous complexes like Pearlman's and Adams' catalysts,[12,13] heavily used in industrial-scale hydrogenation and hydrogenolysis processes, are thought to exhibit exceptional catalytic activity due to the formation of highly reactive M−H bonds on their surface after treatment of these solid state hydroxides and "hydrated oxides" with H_2. Stryker's reagent, a copper hydride complex used in the homogeneous catalysis of conjugate reduction reactions, is typically generated in situ by the hydrogenolysis of Cu−O^{t}Bu bonds.[14] Hydrogenation of metal−formate oxygen bonds is also proposed as the product release step in carbon dioxide reduction to produce formic acid.[15]

It is evident from the examples above that hydrogenolysis of late-transition-metal−oxygen bonds is a fundamental reaction with important consequences in catalysis. This chemical reaction, releasing water or alcohol while producing a metal−hydride, constitutes a powerful combination product release and catalyst regeneration step in a catalytic cycle.[14a,16,17] Many applications of this reaction can be envisioned in the design of new catalytic transformations. Hydrogenation of metal hydroxides generated after oxygen transfer to substrates from metal hydroperoxide species (formed by oxygen insertion into metal−hydride bonds) would allow for oxygenase reactions using molecular oxygen as the oxidant. Catalytic hydrogenation of aldehydes and ketones could similarly involve hydrogenolysis of metal−alkoxide bonds. To fully exploit the unique reactivity of metal−oxygen bonds, however, investigations of mechanism and the scope of the hydrogenolysis reaction are needed. In particular, a mechanistic understanding is essential to developing the ability to select and tune between the competitive reaction pathways (e.g., hydrogenolysis, DBHA) available to metal alkoxides for the effective use of these complexes in catalysis.

Preliminary results on the hydrogenolysis of the pincer palladium(II) hydroxide complex ($^{t\mathrm{Bu}}$PCP)PdOH (**1**, $^{t\mathrm{Bu}}$PCP = 2,6-bis($CH_2P^tBu_2$)C_6H_3) to generate the palladium(II) hydride complex and water were recently reported by us.[9] In this contribution, a broad study investigating the hydrogenolysis of palladium−oxygen bonds is presented using the $^{t\mathrm{Bu}}$PCP pincer framework. The scope of the reaction with respect to hydrogenolysis of various palladium alkoxide and aryloxide linkages is explored. Attemped hydrogenolysis of these compounds to generate alcohol and the corresponding palladium(II) hydride complex ($^{t\mathrm{Bu}}$PCP)PdH (**2**) are described, along with our observations of competitive alternative reaction pathways. The limitations of the hydrogenolysis reaction with respect to steric and electronic considerations of the alkoxide groups are delineated. Kinetic and thermodynamic factors are also addressed. Similar issues of competitive, alternative pathways are likely to be encountered for hydrogenolysis reactions of other metal−heteroatom bonds (e.g., M−N bonds). Thus, results from this study provide broad insight into the application of this reaction step in the design of new transition-metal-catalyzed processes.

RESULTS AND DISCUSSION

($^{t\mathrm{Bu}}$PCP)PdOH. When C_6D_6 solutions of the palladium(II) hydroxide complex ($^{t\mathrm{Bu}}$PCP)PdOH (**1**)[18] were exposed to pressures of hydrogen gas (7.0 atm), room temperature conversion to ($^{t\mathrm{Bu}}$PCP)PdH (**2**) and water was observed over a period of days.[9] The reaction progress was easily monitored by ^{1}H and ^{31}P NMR spectroscopy, and rates were determined by following the disappearance of the methylene signal of **1** as compared to the methyl signal of the internal standard hexamethylbenzene (s, δ = 2.13[19]).

Notably, a few specific resonances in the ^{1}H NMR spectrum for complex **1** shifted upfield during the reaction. This shift can be attributed to the increase in the water concentration due to the formation of water as a product during the reaction. The same upfield shift for **1** was observed in wet C_6D_6 solutions of **1** and was attributed to the interaction between complex **1** and H_2O.[20] Kinetic experiments with different pressures of hydrogen (3.5−7.0 atm) were performed, and in all cases, it was found that the reaction did not follow first-order kinetics in [**1**]. As shown by the example in Figure 1a, plots of ln[**1**] against time do not exhibit linear behavior. In contrast, when the data are plotted

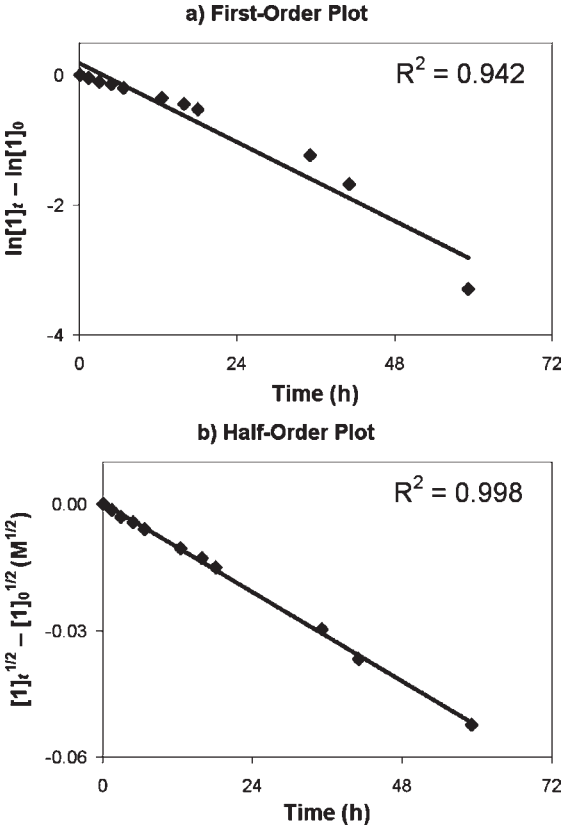

Figure 1. (a) Pseudo-first-order and (b) pseudo-half-order rate plots for the reaction of **1** and H_2 (7.0 atm) in anhydrous C_6D_6 at 25 °C.

Scheme 2

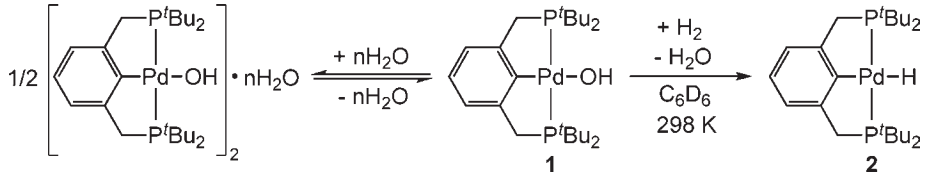

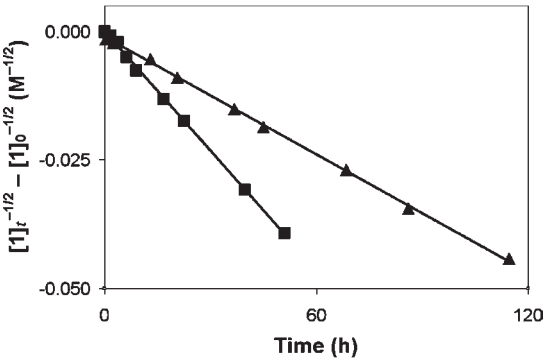

Figure 2. Linear relationship between $[\mathbf{1}]^{1/2}$ and time. Kinetic plots for reactions of **1** with 3.5 atm (▲) and 7.0 atm (■) H_2 in wet C_6D_6 at 25 °C are shown ($[\mathbf{1}]_0$ = 4.2 mM, $[H_2O]_0$ = 38 mM).

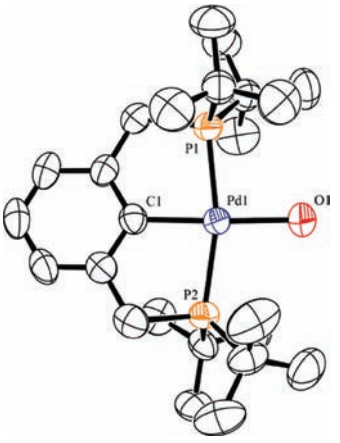

Figure 3. ORTEP of complex ($^{t\mathrm{Bu}}$PCP)PdOH (**1**). Ellipsoids are shown at 50% probability, and hydrogen atoms are omitted for clarity.

of $[\mathbf{1}]^{1/2}$ versus time, excellent correlation to a linear fit is observed (Figure 1b).

Each individual reaction of **1** with H_2 was found to obey half-order kinetics with respect to [**1**] (similar to the example data set shown in Figure 1b). Initially though, the rate constants calculated from the slopes of different kinetic experiments conducted at a given pressure of H_2 were not consistent. However, when excess water (9 equiv)[21] was deliberately added to the reaction solutions, the observed rate constants were highly reproducible, albeit smaller than in the case without added water. At ambient temperature in the presence of excess H_2O, doubling the pressure of H_2 from 3.5 to 7.0 atm effected a doubling of the observed rate constant (Figure 2; k_{obs} = 2.0(1) × 10^{-7} $M^{-1/2}$ s^{-1} to k_{obs} = 4.3(3) × 10^{-7} $M^{-1/2}$ s^{-1}, respectively). This indicates a first-order

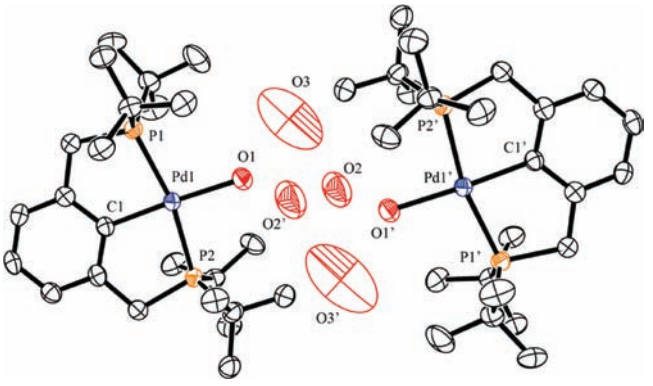

Figure 4. ORTEP of complex $[(^{t\mathrm{Bu}}\mathrm{PCP})\mathrm{PdOH}]_2 \bullet 4H_2O$. Ellipsoids are shown at 50% probability, and hydrogen atoms are omitted for clarity.

dependence of the rate on $[H_2]$.[22] The empirical rate law for the reaction can then be written as $-d[\mathbf{1}]/dt = k_{obs}[H_2][\mathbf{1}]^{1/2}$.

A mechanism involving a dimer−monomer pre-equilibrium prior to rate-determining hydrogenolysis of the monomer (Scheme 2) would be consistent with the unusual half-order dependence on **1**.[23] X-ray structural determinations of the hydroxide complex **1** provide further support. While crystals of **1** grown under rigorously anhydrous conditions afford the monomeric structure shown in Figure 3, crystals of **1** grown in the presence of H_2O revealed a water-bridged dimeric complex $[(^{t\mathrm{Bu}}\mathrm{PCP})\mathrm{PdOH}]_2 \bullet 4H_2O$ (Figure 4).[9] Other PCP-type palladium(II) hydroxides have also been observed to dimerize through bridging water molecules in the solid state.[20,24] Selected bond lengths and angles for both the monomer and dimer are detailed in Table 1. The structural parameters are similar for both forms, with notable elongation of the Pd−O bond from 2.066(3) to 2.094(3) Å when the hydroxide ligand hydrogen-bonds with the bridging water molecules.

The empirical rate law can then be explained by the mechanism shown in eqs 1−2. Hydrogenolysis results from the reaction of the monomeric form of **1** with hydrogen. Formation of the dimeric species inhibits the reaction by removing the reactive monomer from solution. The participation of water in forming the dimer explains the slower rate of reaction observed in the presence of excess water. In addition, this would be consistent with the irreproducibility of the rate constants when excess water was not deliberately added. In this case, differing amounts of adventitious water yield different rates of reaction.

$$2\mathrm{PdOH} + n\mathrm{H_2O} \underset{k_{-1}}{\overset{k_1}{\rightleftharpoons}} [\mathrm{PdOH}]_2 \cdot n\mathrm{H_2O} \qquad (1)$$

$$\mathrm{PdOH} + \mathrm{H_2} \xrightarrow{k_2} \mathrm{PdH} + \mathrm{H_2O} \qquad (2)$$

Assuming that the palladium(II) hydroxide signals observed in the ^{1}H NMR spectra were an average of the signals for the

dx.doi.org/10.1021/ja205824q | J. Am. Chem. Soc. 2011, 133, 17713–17726

Scheme 3

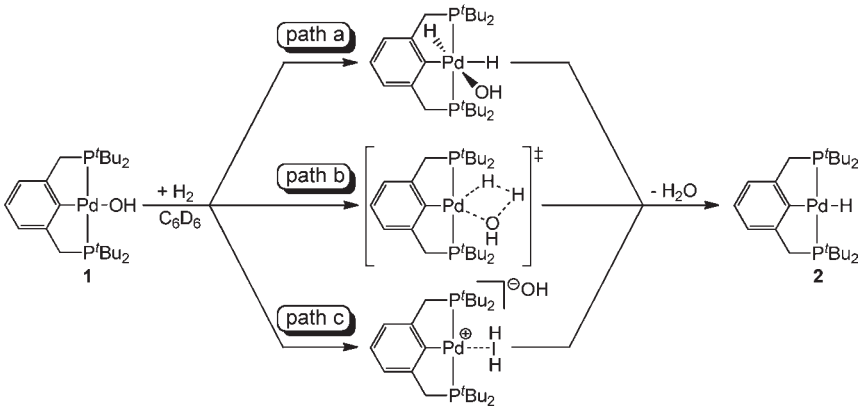

Table 1. Selected Bond Lengths and Angles for Complexes 1 and $[(^{tBu}PCP)PdOH]_2 \cdot 4H_2O$

	1	$[(^{tBu}PCP)PdOH]_2 \cdot 4H_2O$
bond length (Å)		
Pd1−P1	2.2864(11)	2.3027(13)
Pd1−P2	2.2814(11)	2.2991(13)
Pd1−C1	2.022(4)	2.024(4)
Pd1−O1	2.066(3)	2.094(3)
O1•••O2		2.813(4)
O1•••O2′		3.041(4)
bond angle (deg)		
P1−Pd1−P2	166.57(4)	167.06(5)
C1−Pd1−O1	177.30(16)	176.68(17)
C1−Pd1−P1	83.42(12)	83.73(14)
C1−Pd1−P2	83.16(12)	83.63(14)
O1−O2−O1′		100.01(22)
O1−O2′−O1′		100.01(22)

monomer and for the dimer in a fast equilibrium, the total palladium(II) hydroxide concentration can be described as $[PdOH]_{tot} = 2[PdOH]_2 + [PdOH]$. The rate expression for the hydrogenolysis reaction depicted in Scheme 2 and eqs 1−2 was derived in terms of $[PdOH]_{tot}$ (eq 3), with the composite constants $k = k_2/4K'_{eq}$ and $K'_{eq} = k_1[H_2O]^n/k_{-1}$.

$$\text{Rate} = k[H_2]\left(\sqrt{1 + 8K'_{eq}[PdOH]_{tot}} - 1\right) \quad (3)$$

Since eq 3 does not have an easily handled analytical solution, the kinetic data were fitted by numerical integration using the Runge−Kutta fourth-order method.[25] By this method, K'_{eq} for dimer formation (eq 1) was determined to be 1.0 (±0.1) × 10^3 M^{-1} and k_2, the rate constant for the reaction of the monomeric Pd hydroxide with H_2 (eq 2), was 1.5 (±0.3) × 10^{-3} M^{-1} s^{-1}.[26]

Several mechanisms for the key hydrogenolysis step(s) involving the monomeric palladium complex **1** to form **2** and H_2O can be considered. One mechanism (Scheme 3, path **a**) is oxidative addition of H_2 to the Pd^{II}−OH complex to form an octahedral Pd^{IV} intermediate, followed by reductive elimination of H_2O to form **2**. Notably, Pd^{IV} complexes have been reported and significant evidence provided for their involvement as intermediates in Pd^{II} mediated reactions.[27] The second proposed mechanism (Scheme 3, path **b**) involves a four-center transition state wherein a proton is transferred intramolecularly from a coordinated dihydrogen to the oxygen.[28,29] Both of these pathways could proceed via the initial coordination of H_2 to the 16 electron palladium center. Notably, as a cationic dihydrogen complex of the ^{tBu}PCP platinum system is known,[30] a third mechanism (Scheme 3, path **c**) would be the dissociation of the OH^- ligand, H_2 coordination, and deprotonation by the resulting OH^- to form water and the Pd^{II}−H. However, if hydroxide dissociation were involved as a preliminary step, the addition of excess water to the reaction would be expected to increase,[31] rather than decrease, the rate of reaction as was confirmed experimentally.

In the absence of observable intermediates, it is challenging to experimentally distinguish between the remaining two pathways. Computational methods (B3LYP density functional theory[32]) were then employed to compare the energetics of the pathways. As illustrated in Figure 5 for a model PCP complex, the four-center transition state (**B**) was found to be significantly lower in energy than the oxidative addition intermediate (**A**). Notably the involvement of the oxygen lone pair in the four-center transition state distinguishes path **B** from a true σ-bond metathesis, and this type of intramolecular proton transfer has been termed internal electrophilic substitution (IES).[29]

Our experimental and computational studies of the hydrogenolysis reaction of **1** are consistent with the concerted reaction of hydrogen with a monomeric d^8 metal center and the lone pair of the hydroxide oxygen. Similar reactivity should be expected for monomeric d^8 metal alkoxides and aryloxides with hydrogen. In fact, one might anticipate that hydrogenolysis of metal alkoxide or aryloxide species should be more straightforward as the tendency to dimerize through bridging water and/or alcohol molecules would be less significant. Both the sterics of the alkoxide or aryloxide substituent and the lack of a hydrogen bound to oxygen should inhibit hydrogen-bonded dimerization. In a broader context, the study of hydrogenolysis of the alkoxide and aryloxide analogues enables us to investigate the generality of hydrogenolysis reactions with respect to a range of M−O bonds. A greater understanding of the scope of this reaction will allow for its successful application in catalysis.

(^{tBu}PCP)PdOCH$_3$. The first palladium(II) alkoxide species targeted was the methoxide complex (^{tBu}PCP)PdOCH$_3$ (**3**).[9] It was quickly discovered, however, that complex **3** is extremely

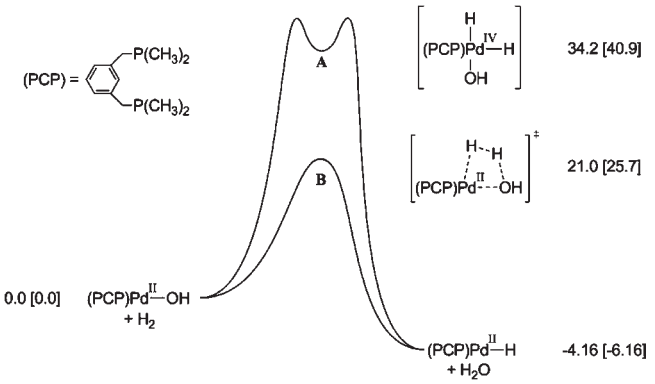

Figure 5. Energies (ΔH [ΔG]) are in kcal mol^{-1} for gas phase species. **A** corresponds to the Pd^{IV} intermediate for the oxidative addition/reductive elimination pathway, and **B** to the transition state for the four-center intramolecular proton transfer. PCP = ^{Me}PCP (2,6-bis($CH_2P(CH_3)_2$)C_6H_3).

Scheme 4

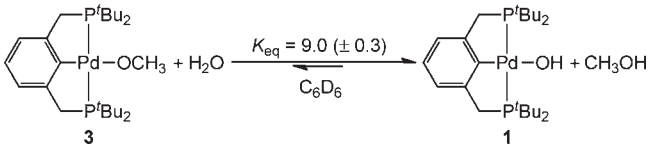

sensitive to adventitious water. Notably, dimerization was not the culprit but rather hydrolysis. Upon deliberate exposure of **3** (19 mM) in benzene-d_6 to water (8.0 mM), rapid conversion to the hydroxide complex **1** and the release of methanol were clearly observed by ^{1}H and ^{31}P NMR spectroscopy. To probe the equilibrium between these two palladium species, a benzene-d_6 solution of the methoxide complex **3** was treated with 0.5 equiv of H_2O, and the change in concentration between complexes **3** and **1** was monitored by ^{1}H NMR spectroscopy over the course of 5 h. Using eq 4 and the concentrations of **1**, **3**, methanol, and water[33] calculated against an internal hexamethylbenzene standard, an equilibrium constant (K_{eq}) of 9.0 (±0.3) was obtained (Scheme 4). Thus, when 1 equiv of methanol was added to a benzene-d_6 solution of the hydroxide complex **1**, only a small percentage of complex **3** (<10%) was observed by NMR spectroscopy. Clearly, the reaction of **3** with H_2O favors the production of **1** and methanol. This result is consistent with other examples in the literature where a late-transition-metal alkoxide complex undergoes hydrolysis to generate a hydroxide ligand and the corresponding alcohol.[10,34,35]

$$K_{eq} = [PdOH][CH_3OH]/[PdOCH_3][H_2O] \quad (4)$$

Analogous to the hydrogenolysis reaction observed with the hydroxide complex **1**, exposure of the methoxide complex **3** to dihydrogen (7.0 atm) in C_6D_6 yields the palladium(II) hydride complex **2** and methanol over a period of 80 h at room temperature in 96% yield, as determined by ^{1}H and ^{31}P{^{1}H} NMR spectroscopy.[9] However, the rate for hydrogenolysis of **3** was not reproducible. Given the results described above for the hydrogenolysis reaction of the Pd hydroxide complex **1**, it is reasonable to suggest that adventitious H_2O is responsible for the irreproducibility. Notably, even when extreme care was taken to maintain anhydrous conditions, a small amount of the hydroxide complex **1** was always observed in the hydrogenolysis reactions of palladium methoxide complex **3**, indicative of the presence of adventitious water. Furthermore, the hydroxide complex **1**, the hydrolysis product of **3**, will also undergo hydrogenolysis to form the palladium hydride complex **2**.

Scheme 5. Two Possible Paths for the Conversion of (^{tBu}PCP)PdOR and H_2 to (^{tBu}PCP)PdH and ROH (R ≠ H)

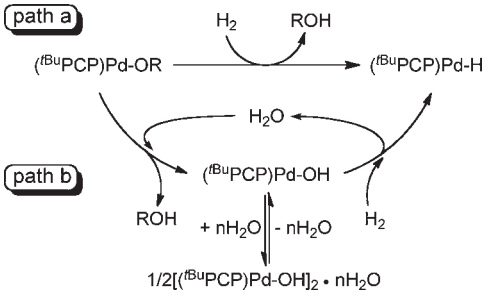

Avoiding the hydrolysis reaction is critical to achieving reproducible kinetics for the hydrogenolysis of complex **3**. As illustrated in Scheme 5, the presence of H_2O during a hydrogenolysis reaction actually leads to the production of the same products through two competing pathways **a** and **b**. Acting as a catalyst for path **b**, H_2O converts the alkoxide complex to the hydroxide complex, which then reacts with hydrogen to regenerate water. Both pathways have indistinguishable products, as both yield alcohol and complex **2**. Yet, the order of the reaction with respect to [Pd] would be different for the two mechanisms (i.e., first- and half-order in [Pd] for path **a** and **b**, respectively). In addition, the rate constant for the hydrogenolysis of the monomeric palladium hydroxide and the palladium methoxide is also likely to be different. Thus, if path **b** is active to different extents based on adventitious water, obtaining reproducible kinetics would be challenging.

Adding excess methanol to the methoxide system should shift the equilibrium in Scheme 4 in favor of the methoxide complex **3**. However, the addition of methanol resulted in promotion of a different type of reaction. As illustrated in Scheme 6, the presence of CH_3OH assists in the conversion of complex **3** to the hydride complex **2** through an alcohol-promoted dissociative β-hydride abstraction (DBHA) mechanism. When 10 equiv methanol were added to C_6D_6 solutions of **3** in the absence of H_2, complete conversion to the hydride complex **2** at room temperature was observed over 3 days. DBHA has been reported for other late-transition-metal systems[11,35,36] and is distinct from the traditional β-hydride elimination of metal alkyls. The DBHA pathway proceeds through the heterolytic dissociation of the alkoxide anion, producing a (^{tBu}PCP)Pd cation. Hydride abstraction from the alkoxide anion leads to **2** and formaldehyde. The addition of methanol accelerates this reaction path by stabilizing the alkoxide anion through hydrogen bonding and thus assisting in the alkoxide dissociation.

Methanol-free solutions of **3** in benzene-d_6 are relatively stable at ambient temperatures in the absence of H_2. Only a small percentage (<10%) of **3** was observed to decompose over the course of 1 week at room temperature. A similar amount of the hydride complex **2** was formed during this period, yet no methanol production was detected by ^{1}H NMR spectroscopy. At 65 °C, however, complete conversion of **3** to **2** (80%) and a

Scheme 6

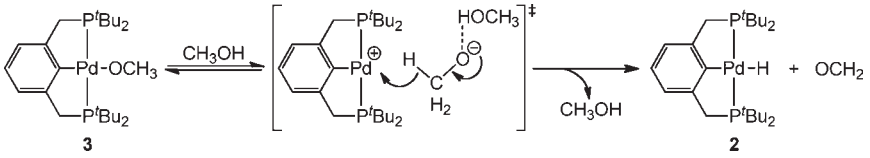

Scheme 7

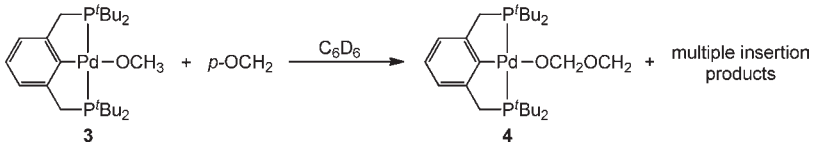

Scheme 8

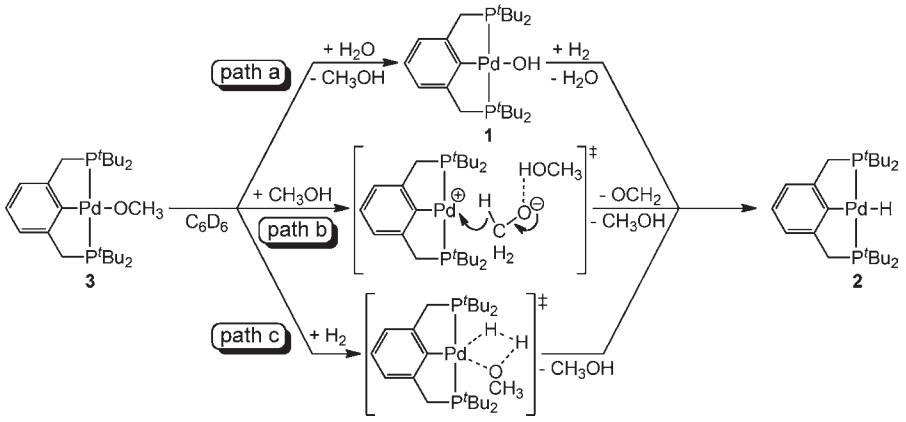

new minor species (20%) was observed in 15 h. The minor species has a very similar ^{1}H NMR spectrum to complex **3** with an additional resonance at 5.72 ppm that integrates to two protons. In analogy to reactivity observed in a Pt(IV)−OCH_3 system[35] and consistent with formaldehyde as a product in the DBHA reaction of complex **3**, this new species is proposed to be the OCH_2 insertion product ($^{t\mathrm{Bu}}$PCP)PdOCH_2OCH_3 (**4**). To confirm the identity of complex **4** as well as to establish the probable pathway for its production, the palladium(II) methoxide complex **3** was allowed to react with *para*-formaldehyde (10 equiv) to provide an independent synthesis of **4** (Scheme 7). Within minutes of dissolving the two reagents together in C_6D_6 at room temperature, partial conversion of **3** to **4** was observed by NMR spectroscopy. The complete disappearance of **3** was observed after 30 min, and the presence of complex **4** along with other Pd species was detected by NMR spectroscopy. Similar to the Pt system,[35] the additional products are most likely the result of multiple OCH_2 insertions.

The seemingly subtle modification from Pd−OH to −OCH_3 effects a significant change in reactivity between the two metal complexes. While the addition of a methoxide moiety adds steric encumbrance that can be expected to inhibit dimerization, the new palladium(II) species **3** is also extremely sensitive to hydrolysis, leading to formation of the hydroxide complex **1** (Scheme 8, path **a**). The addition of methanol to solutions of complex **3** in an attempt to suppress hydrolysis instead resulted in the promotion of the DBHA reaction pathway (Scheme 8, path **b**). While the hydrogenolysis of complex **3** was observed to occur (Scheme 8, path **c**), the competing hydrolysis and DBHA reactions, which ultimately also result in the formation of the same hydride complex **2**, made kinetic studies and a valid comparison to the hydroxide system impractical. To investigate hydrogenolysis reactions of palladium alkoxides in greater detail, PdOR complexes resistant to hydrolysis and to DBHA reactivity are needed. Alkoxide ligands that either lack β-hydrogens or are too bulky to undergo the rearrangement necessary for the DBHA mechanism should be considered as viable candidates.

($^{t\mathrm{Bu}}$PCP)PdOC_6H_5. As a phenoxide group lacks β-hydrogens necessary for a competitive DBHA pathway, the palladium(II) phenoxide complex ($^{t\mathrm{Bu}}$PCP)PdOC_6H_5 (**5**) was prepared. Complex **5** was synthesized by a procedure analogous to that of **3**, in which the nitrate complex, ($^{t\mathrm{Bu}}$PCP)PdONO_2, was mixed with potassium phenoxide in THF (Scheme 9). The phenoxide complex was characterized by NMR spectroscopy, elemental analysis, and X-ray crystallography. The ORTEP of **5** is shown in Figure 6, exhibiting the square planar geometry expected for a palladium(II) species, and selected bond lengths and angles are presented in Table 2. Of note, the Pd−O bond for **5** (2.0900(12) Å) is just slightly longer than that in the methoxide complex **3** (2.084(3) Å).[9]

dx.doi.org/10.1021/ja205824q |*J. Am. Chem. Soc.* 2011, 133, 17713–17726

Scheme 9

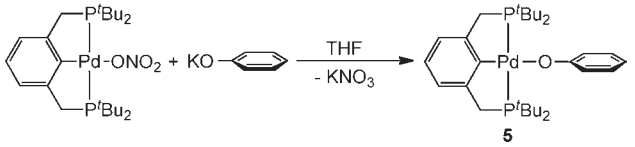

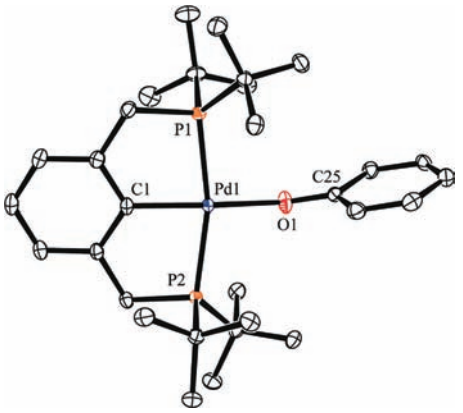

Figure 6. ORTEP of complex ($^{t\mathrm{Bu}}$PCP)PdOC$_6$H$_5$ (**5**). Ellipsoids are shown at 50% probability, and hydrogen atoms are omitted for clarity.

Table 2. Selected Bond Lengths and Angles for Complex 5

bond length	Å	bond angle	deg
Pd1–P1	2.3161(4)	P1–Pd1–P2	164.605(15)
Pd1–P2	2.2931(4)	C1–Pd1–O1	163.94(6)
Pd1–C1	2.0061(15)	C1–Pd1–P1	83.66(5)
Pd1–O1	2.0900(12)	C1–Pd1–P2	97.82(4)
O1–C25	1.3110(19)	Pd1–O1–C25	137.20(11)

Notably when an excess of H_2O (280 mM) was added to a benzene-d_6 solution of the phenoxide complex **5** (6.5 mM) and heated to 125 °C for 1 day, no reaction was detected by NMR spectroscopy. The lack of reactivity with water indicates that adventitious water is unlikely to affect the hydrogenolysis reaction. However, when **5** was treated with H_2 gas (7.0 atm) at room temperature, the conversion to the hydride complex **2** and free phenol was observed to only reach 20% completion after 2 weeks. The reaction was monitored for an additional week, but the conversion of **5** to **2** appeared to halt at 20%. It was suspected that the reaction had reached equilibrium. Consistent with this proposal, when a C_6D_6 solution of the palladium(II) hydride complex **2** (20 mM) was exposed to phenol (40 mM), rapid bubbling occurred and the conversion of **2** to **5** was observed by ^{1}H and ^{31}P NMR spectroscopies. Over time, faint-yellow crystals grew out of solution, which were characterized by X-ray crystallography as the dimeric Pd(0) complex [(μ-$^{t\mathrm{Bu}}$PCHP)Pd]$_2$ (**6**, Figure 7). Complex **6** contains the bridging ligand α,α'-bis(di-*tert*-butylphosphino)-*m*-xylene ($^{t\mathrm{Bu}}$PCHP), and precedent for this type of alcohol-promoted reduction of Pd(II) complexes has been observed in the analogous $^{i\mathrm{Pr}}$PCP system.[37]

($^{t\mathrm{Bu}}$PCP)PdOCH$_2$C(CH$_3$)$_3$. As demonstrated above, the phenoxide complex ($^{t\mathrm{Bu}}$PCP)PdOC$_6$H$_5$ (**5**) does not undergo hydrogenolysis but instead the reverse reaction. Protonation of the

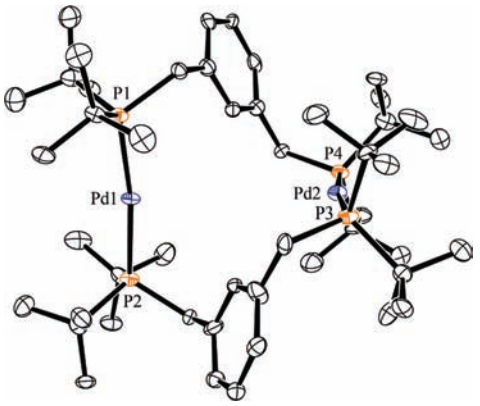

Figure 7. ORTEP of dimeric complex [(μ-$^{t\mathrm{Bu}}$PCHP)Pd]$_2$ (**6**). Ellipsoids are shown at 50% probability, and hydrogen atoms are omitted for clarity. Selected bond lengths (Å) and angles (deg): Pd1–P1, 2.271(2); Pd1–P2, 2.265(3); P1–Pd1–P2, 171.78(10).

Scheme 10

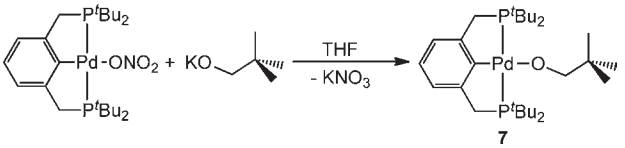

hydride complex **2** with phenol to liberate hydrogen and generate **5** is thermodynamically favored. Given that phenols are considerably more acidic (pK_a = 7–10) than alcohols (pK_a = 16–20),[38] the thermodynamics of hydrogenolysis may be more favorable for alcohols. A palladium neopentoxide complex could provide for a favorable hydrogenolysis, and although the neopentoxide ligand contains β-hydrogens, its steric bulk should make it difficult to align its β-hydrogens for DBHA. Therefore, as shown in Scheme 10, the palladium(II) neopentoxide complex ($^{t\mathrm{Bu}}$PCP)PdOCH$_2$C(CH$_3$)$_3$ (**7**) was prepared from the Pd(II) nitrate and potassium neopentoxide. Complex **7** was fully characterized by NMR spectroscopy, elemental analysis, and X-ray crystallography. The ORTEP is shown in Figure 8, and selected bond distances and angles are reported in Table 3. Like complex **5**, a typical square planar geometry is observed in the solid state for the Pd(II) complex **7**. Additionally, the Pd–O bond length for **7** (2.081(2) Å) is similar to that in the methoxide complex **3** (2.084(3) Å)[9] and phenoxide complex **5** (2.0900(12) Å) and slightly longer than that in the hydroxide complex **1** (2.066(3) Å)

The palladium(II) neopentoxide complex did not undergo DBHA even when solutions of **7** were heated to 150 °C in the presence of excess neopentyl alcohol. Surprisingly, however, there was no reaction of complex **7** with dihydrogen (7.0 atm), even at temperatures exceeding 100 °C. This result was unexpected, especially since the Pd–O bond distances for **7** and the methoxide complex **3** are so similar. As the electronics of the two alkoxides are likely to be similar, the lack of reactivity may be attributed to the increase in steric bulk of the neopentoxide group. Examination of the space-filling diagram[39] reveals limited access to the palladium and oxygen atoms due to the large size of the *tert*-butylphosphino groups combined with that of the neopentoxide

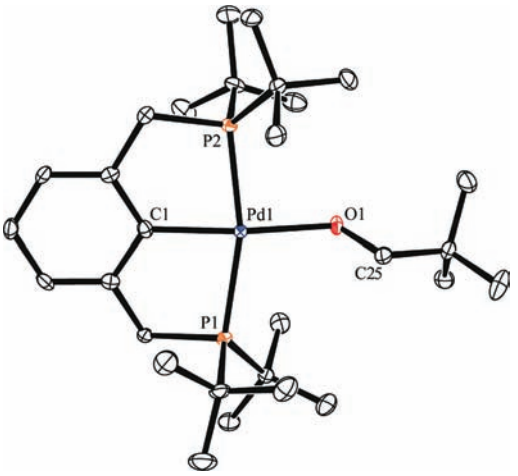

Figure 8. ORTEP of complex ($^{t\mathrm{Bu}}$PCP)PdOCH$_2$C(CH$_3$)$_3$ (**7**). Ellipsoids are shown at 50% probability, and hydrogen atoms are omitted for clarity.

Table 3. Selected Bond Lengths and Angles for Complex 7

bond length	Å	bond angle	deg
Pd1−P1	2.3247(8)	P1−Pd1−P2	165.17(3)
Pd1−P2	2.2853(8)	C1−Pd1−O1	171.99(10)
Pd1−C1	2.023(3)	C1−Pd1−P1	83.02(9)
Pd1−O1	2.081(2)	C1−Pd1−P2	82.20(9)
O1−C25	1.383(3)	Pd1−O1−C25	123.99(18)

ligand. As discussed above, involvement of both the Pd center and the lone pair on the oxygen was implicated for the hydrogenolysis reaction of the palladium(II) hydroxide complex **1**.

($^{t\mathrm{Bu}}$PCP)PdOCH$_2$CF$_3$ and ($^{t\mathrm{Bu}}$PCP)PdOCH$_2$CHF$_2$. Palladium complexes with fluorinated ethoxide ligands should have less steric bulk than the neopentoxide analog, and the terminal electron-withdrawing groups (EWG) should deter a potential DBHA decomposition pathway. The DBHA pathway would be disfavored from the metal alkoxide complex with analogy to the equilibrium behavior between aldehydes and their corresponding hydrates (Scheme 11a). The addition of terminal EWG to aldehydes causes a shift in equilibrium toward sp^3 hybridized hydrates over sp^2 hybridized aldehydes.[40] The same trend should apply to sp^3 hybridized alkoxide ligands and sp^2 hybridized aldehydes (Scheme 11b). An alkoxide ligand containing terminal electron-withdrawing fluorine atoms should therefore be more resistant to DBHA (i.e., conversion to sp^2 hybridized aldehyde products).

The palladium(II) 2,2,2-trifluoroethoxide complex ($^{t\mathrm{Bu}}$PCP)-PdOCH$_2$CF$_3$ (**8**) and the palladium(II) 2,2-difluoroethoxide complex ($^{t\mathrm{Bu}}$PCP)PdOCH$_2$CHF$_2$ (**9**) were prepared. Notably, however, 2,2,2-trifluoroethanol (TFE, pK_a = 12.4) and 2,2-difluoroethanol (DFE, pK_a = 13.3) are fairly acidic.[41] Thus, reaction of the hydride complex **2** with TFE or DFE to release H$_2$ and produce the palladium alkoxide, analogous to the reaction observed for **2** with phenol, might be expected. Indeed, the reaction of a C$_6$D$_6$ solution of **2** (15.0 mM) with an excess of TFE (175 mM) resulted in the complete conversion to **8** and hydrogen within seconds (Scheme 12), as observed by NMR spectroscopy. The methylene resonance for the 2,2,2-trifluoroethoxide ligand in complex **8** appears in the ^{1}H NMR spectrum

Scheme 11

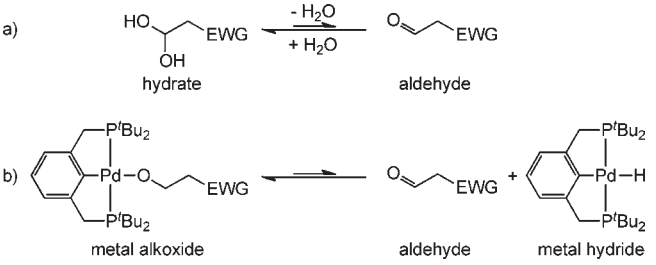

Scheme 12

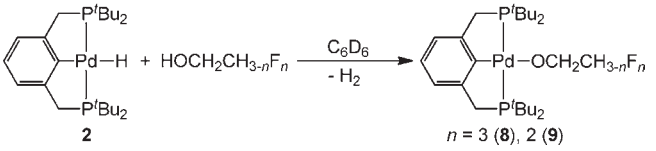

as a quartet at 4.65 ppm ($^3J_{HF}$ = 9.9 Hz), and the ^{19}F NMR spectrum contains a triplet at −73.3 ppm ($^3J_{FH}$ = 9.9 Hz). Similarly, treatment of a C$_6$D$_6$ solution of **2** (15.0 mM) with DFE (198 mM) resulted in the formation of **9** and hydrogen. The methyl proton on the 2,2-difluoroethoxide ligand (C*H*F$_2$) of **9** appears as a characteristic triplet of triplets at 6.07 ppm ($^2J_{HF}$ = 58.0 Hz, $^3J_{HH}$ = 4.2 Hz), and the methylene protons (C*H*$_2$CHF$_2$) are observed as a triplet of doublets at 4.51 ppm - ($^3J_{HF}$ = 15.2 Hz, $^3J_{HH}$ = 4.2 Hz) in the ^{1}H NMR spectrum. In the ^{19}F NMR spectrum, complex **9** displays a doublet of triplets at −124.5 ppm ($^2J_{FH}$ = 58.0 Hz, $^3J_{FH}$ = 15.2 Hz). Of note, the conversion of **2** to **9** with DFE was significantly slower than the reaction of **2** and TFE, requiring several hours to reach completion as compared to seconds for formation of **8** (Scheme 12). The complete conversion of these reactions of **2** with TFE or DFE to produce the corresponding palladium alkoxide indicates the thermodynamics of hydrogenolysis of the palladium alkoxide are unfavorable, similar to the situation observed with the palladium phenoxide complex.

($^{t\mathrm{Bu}}$PCP)PdOCH$_2$CH$_2$F. The trend of decreasing acidity with the decrease in the number of terminal fluorine atoms on the series of fluoroethanols prompted the investigation of the reactivity of 2-fluoroethanol (FE, pK_a = 14.4)[42] with the palladium hydride complex. When an excess of FE (213 mM) was exposed to a C$_6$D$_6$ solution of complex **2** (15.0 mM) at room temperature, no conversion to ($^{t\mathrm{Bu}}$PCP)PdOCH$_2$CH$_2$F (**10**) was observed over the course of 2 weeks.

An independent synthesis of complex **10** was next attempted following the analogous preparations for complexes **3**, **5**, and **7**. Unfortunately, the potassium reagent KOCH$_2$CH$_2$F could not be prepared through the reaction of FE and potassium metal. Instead, a highly viscous mixture of several products was obtained. Therefore, an alternate route involving the displacement of the neopentoxide ligand of complex **7** with FE was used (Scheme 13). This reaction yielded complex **10** and an equivalent of neopentyl alcohol (NpOH). The NpOH was then removed under reduced pressure, and complex **10** was isolated and characterized by NMR spectroscopy. The ^{19}F NMR spectrum for complex **10** contains a triplet of triplets at −218.6 ppm ($^2J_{FH}$ = 48.7 Hz, $^3J_{FH}$ = 21.3 Hz), and the ^{1}H NMR

Scheme 13

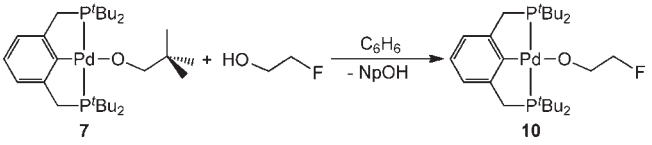

Scheme 14

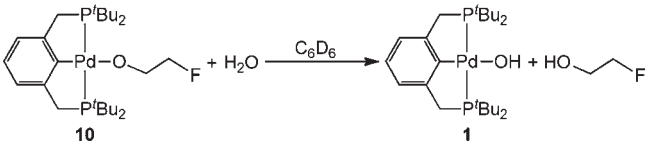

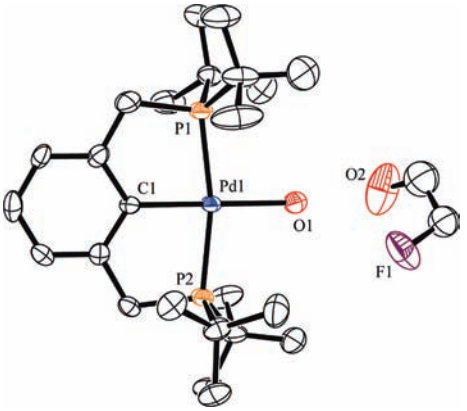

Figure 9. ORTEP of complex ($^{t\mathrm{Bu}}$PCP)PdOH•HOCH$_2$CH$_2$F (**1•FE**). Ellipsoids are shown at 50% probability, and hydrogen atoms are omitted for clarity.

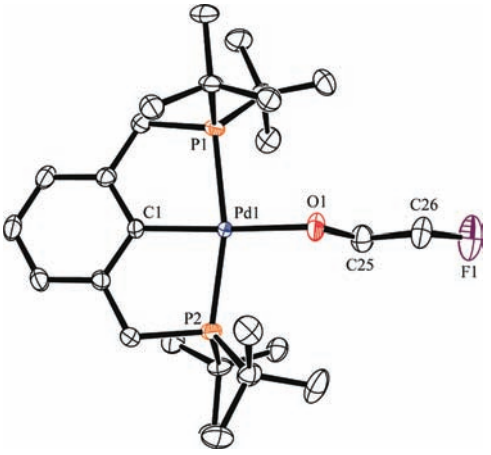

Figure 10. ORTEP of complex ($^{t\mathrm{Bu}}$PCP)PdOFE (**10**). Ellipsoids are shown at 50% probability, and hydrogen atoms are omitted for clarity.

Table 4. Selected Bond Lengths and Angles for Complex 1•FE

bond length	Å	bond angle	deg
Pd1–P1	2.285(2)	P1–Pd1–P2	166.61(9)
Pd1–P2	2.280(2)	C1–Pd1–O1	179.1(4)
Pd1–C1	1.996(8)	C1–Pd1–P1	84.0(2)
Pd1–O1	2.090(6)	C1–Pd1–P2	83.6(2)
O1•••O2	2.602(11)	Pd1–O1•••O2	157.89(13)
O1•••F1	3.011(11)	Pd1–O1•••F1	141.76(13)

Table 5. Selected Bond Lengths and Angles for Complex 10

bond length	Å	bond angle	deg
Pd1–P1	2.2996(8)	P1–Pd1–P2	166.45(3)
Pd1–P2	2.2965(8)	C1–Pd1–O1	172.38(11)
Pd1–C1	2.021(3)	C1–Pd1–P1	83.01(8)
Pd1–O1	2.082(2)	C1–Pd1–P2	83.44(8)
O1–C25	1.361(4)	Pd1–O1–C25	129.2(2)
C26–F1	1.375(4)	C25–C26–F1	113.3(3)

resonance for the $-CH_2F$ protons appears at 4.78 ppm as a doublet of triplets ($^2J_{HF}$ = 48.7 Hz, $^3J_{HH}$ = 5.7 Hz).

Highlighting the hygroscopic nature of these alkoxide complexes, an attempt to grow X-ray quality crystals of ($^{t\mathrm{Bu}}$PCP)-PdOCH$_2$CH$_2$F by slow diffusion of pentane into a concentrated benzene solution of **10** instead resulted in the hydroxide complex **1** with an associated fluoroethanol ($^{t\mathrm{Bu}}$PCP)PdOH•HOCH$_2$CH$_2$F (**1•FE**, Figure 9). Examination of the crystallographic data in Table 4 reveals that the Pd–O bond length in complex **1•FE** is significantly elongated (2.090(6) Å) as compared to complex **1** (2.066(3) Å), indicative of electron donation from the hydroxide ligand to FE through hydrogen bonding. Presumably, an equivalent of H_2O was introduced during crystallization, displacing the 2-fluoroethoxide ligand of complex **10** (Scheme 14), thus converting the alkoxide complex to **1** and FE. This chemistry is very similar to that described above for the methoxide complex **3** in the presence of water where conversion to the hydroxide complex **1** and methanol was favored.

In a separate experiment being extremely careful to avoid H_2O contamination, complex **10** was successfully isolated and characterized by elemental analysis and X-ray crystallography. As illustrated in Figure 10, the ORTEP of complex **10** exhibits the same square planar geometry observed for its palladium alkoxide analogues, and the Pd1–O1 bond length is also comparable at 2.082(2) Å (Table 5).

In the absence of water, solutions of complex **10** in C_6D_6 are extremely stable, even in the presence of excess FE. Notably, the ^{1}H NMR resonances for **10** do not shift in varying concentrations of FE, suggesting that no significant hydrogen bonding between complex **10** and FE is occurring in solution. As a control, an NMR tube was prepared with a C_6D_6 solution of **10** and 9 equiv of FE. In the absence of H_2, the sample was heated to 60 °C in a temperature-controlled oil bath for 7 days. By ^{1}H NMR spectroscopy, < 5% conversion of complex **10** to the hydride complex **2** through DBHA was observed. Notably, virtually complete conversion of the analogous methoxide complex **3** to **2** by DBHA occurs in 15 h under similar conditions. Thus **10** shows a significantly reduced proclivity for the DBHA pathway as compared with complex **3**. The stability of **10** toward DBHA and the lack of interaction with FE allows for kinetic studies of the hydrogenolysis reaction in the presence of excess FE, which is needed to prevent hydrolysis by adventitious water (see Scheme 5).

dx.doi.org/10.1021/ja205824q |*J. Am. Chem. Soc.* 2011, 133, 17713–17726

Scheme 15

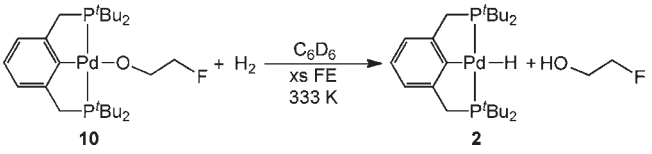

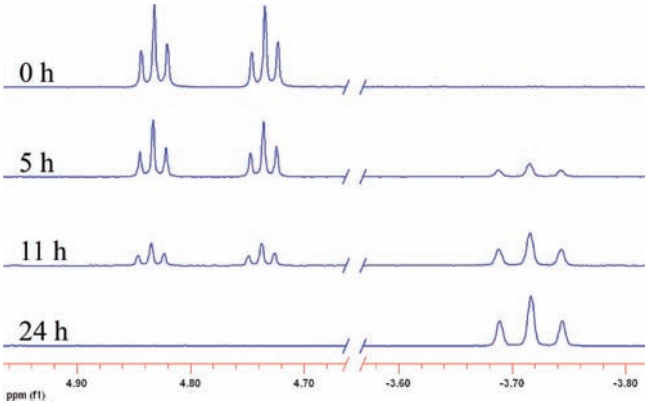

Figure 11. Partial ^{1}H NMR spectra for the reaction of **10** (3.6 μmol) and H_2 (7.0 atm) in C_6D_6 with excess FE (32 μmol) at 60 °C over a period of 24 h. The disappearance of the $-CH_2CH_2F$ signal for **10** (doublet of triplets, ca. 4.78 ppm) is observed along with the appearance of the Pd—*H* signal for **2** (virtual triplet, ca. −3.72 ppm).

The addition of H_2 (7.0 atm) to a benzene-d_6 solution of the palladium 2-fluoroethoxide complex **10** at room temperature in the presence of excess FE (9 equiv) resulted in the quantitative conversion to the palladium hydride complex **2** and FE over the course of nearly 1 month. At 60 °C, however, the reaction reaches completion within 24 h (Scheme 15).

The reaction progress at 60 °C was monitored by NMR spectroscopy; in the ^{1}H NMR spectrum, the disappearance of the $-CH_2F$ resonance for **10** was observed along with the appearance of the Pd—*H* resonance for **2** (Figure 11). It was found that each individual reaction of **10** with excess H_2 (in the presence of excess FE) at 60 °C obeyed a pseudo-first-order rate dependency with respect to [**10**], exhibiting an excellent linear fit to the data (Figure 12a). By contrast, plots of $[\mathbf{10}]^{1/2}$ against time are clearly not linear (Figure 12b).[43] Doubling the partial pressure of H_2 from 3.5 to 7.0 atm resulted in a doubling of the observed rate constant (1.5 (±0.4) × 10^{-5} s^{-1} to 3.4 (±0.2) × 10^{-5} s^{-1}, respectively), indicating a first-order rate dependence in [H_2] (Figure 13). Thus the empirical rate law for the hydrogenolysis of **10** is $-d[\mathbf{10}]/dt = k_{obs}[H_2][\mathbf{10}]$.

Notably, when hydrogenolysis reactions of **10** were performed in the absence of excess FE, small amounts of the hydroxide complex **1** were consistently observed by NMR spectroscopy as a contaminant. The presence of **1** is an indication of the sensitivity of complex **10** to hydrolysis by adventitious H_2O. It was generally observed that the experiments in which higher concentrations of **1** were detected were also noted to yield faster reaction times. These reactions also exhibited deviations from the first-order reaction dependency in [**10**]; however, the data did not fit half-order kinetics either. This kinetic behavior would be consistent with the simultaneous operations of paths **a** and **b** (Scheme 5), with the contribution of path **b** depending on the concentration

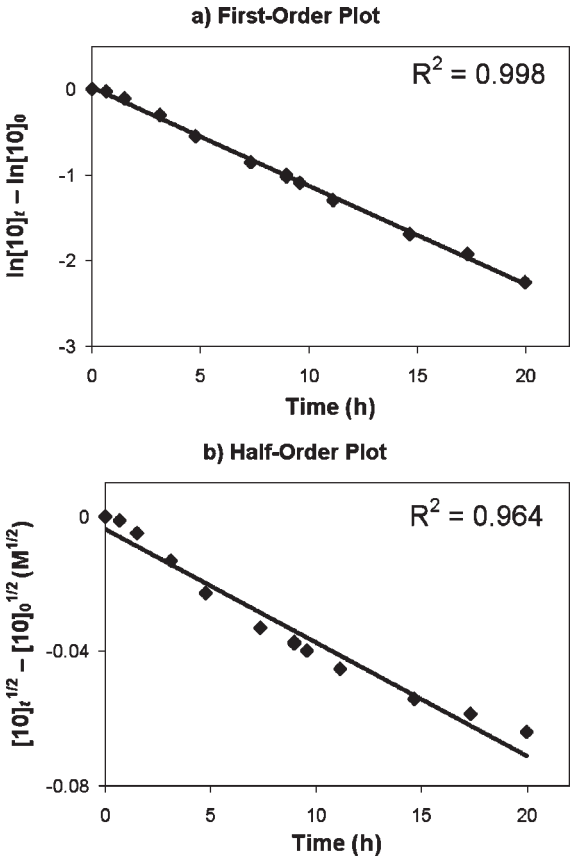

Figure 12. (a) Pseudo-first-order and (b) pseudo-half-order rate plots for the reaction of **10** (3.6 μmol) and H_2 (7.0 atm) in C_6D_6 with excess FE (32 μmol) at 60 °C.

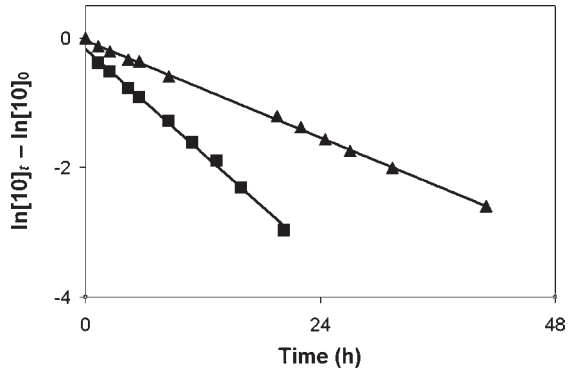

Figure 13. Linear relationship between ln[**10**] and time. Kinetic plots for reactions of **10** (3.6 μmol) with 3.5 atm (▲) and 7.0 atm (■) H_2 in C_6D_6 with excess FE (32 μmol) at 60 °C are shown.

of adventitious water available to generate **1**. In this situation, the palladium hydride complex **2** can be formed from the hydrogenolyses of both complexes **10** and **1**. In path **b**, H_2O acts as a catalyst, hydrolyzing the alkoxide complex to the hydroxide complex **1**, which then reacts with hydrogen to regenerate water. The perturbation from first-order kinetics is attributed to the dimer formation that takes place for **1** as discussed above. In contrast, when an excess of FE is present during hydrogenolysis reactions of the 2-fluoroethoxide complex

dx.doi.org/10.1021/ja205824q |*J. Am. Chem. Soc.* 2011, 133, 17713–17726

10, the hydrolysis of **10** is inhibited, and the hydrogenolysis of **10** primarily proceeds via path **a** in Scheme 5.[44]

The empirical rate law for the hydrogenolysis of **10**, determined with excess FE present, shows a first-order dependence on [**10**] and a first-order dependence on [H_2], and is thus consistent with a mechanism analogous to that proposed for the Pd−OH monomer (eq 5). Interaction of H_2 with the Pd center and the lone pair of the oxygen leads directly to the Pd−H and O−H bond formations. Thus, once the competing reactions of dimerization, hydrolysis, and DBHA are inhibited, hydrogenolysis of Pd−O bonds of hydroxide and alkoxide complexes was found to occur via a common mechanism.

$$PdOCH_2CH_2F + H_2 \xrightarrow{k} PdH + HOCH_2CH_2F \qquad (5)$$

SUMMARY

Comparison of the reactivity of palladium(II) hydroxide, alkoxide, and phenoxide complexes with hydrogen has revealed a range of reactions. Whether hydrogenolysis, β-hydride abstraction, hydrolysis (by adventitious water), or even a lack of reaction was observed, the reactivity was found to be controlled by the basicity of the −OR group, its steric bulk, and its susceptibility to a dissociative β-hydride abstraction pathway. Hydrogen reacts directly with the hydroxide complex **1** to generate water and the palladium(II) hydride complex **2**. This hydrogenolysis reaction is retarded by dimer formation involving hydrogen-bonded water molecules. Hydrogenolysis occurs with the monomeric d^8 metal species through an internal electrophilic substitution (IES) mechanism (Scheme 3). A similar direct hydrogenolysis occurs with the palladium(II) methoxide complex **3** to generate the hydride complex **2** and methanol. However detailed kinetic and mechanistic studies of the hydrogenolysis of **3** could not be performed due to a competing hydrolysis by adventitious water which forms the hydroxide complex **1**. Addition of excess methanol to thwart hydrolysis results in a rapid dissociative β-hydride abstraction (DBHA) reaction that also produces the hydride complex **2**.

The palladium(II) neopentoxide complex **7** was also synthesized. Notably this complex was found to be stable to DBHA, even in the presence of added neopentanol at elevated temperatures. The sterics of the neopentyl group apparently hinder the DBHA reaction. However, the sterics of the neopentoxide ligand, combined with the sterics of the ^{t}Bu groups on the phosphine, also inhibit reaction with hydrogen, and no hydrogenolysis was observed.

The reactivity of the palladium(II) phenoxide complex **5**, 2,2,2-trifluoroethoxide complex **8**, and 2,2-difluoroethoxide complex **9** with hydrogen was limited. In these cases, thermodynamics are the main consideration as the palladium alkoxide complexes and H_2 are favored over the palladium(II) hydride complex **2** and alcohol products. This preference was convincingly demonstrated by the reaction of the hydride complex **2** with the alcohol. Notably the alcohols in question (i.e., phenol, TFE, and DFE) are all quite acidic, with pK_a values of 9.95, 12.4, and 13.3, respectively.[38,41] FE is less acidic with a pK_a of 14.4, and the equilibrium in this case favored the hydride. Thus similar to the palladium hydroxide **1** and the palladium methoxide **3**, the palladium(II) 2-fluoroethoxide complex **10** undergoes hydrogenolysis. The reaction of **10** with hydrogen produces the palladium(II) hydride and FE. The fluorine substitution disfavors a DBHA reaction, and kinetic studies of the hydrogenolysis could be carried out in the presence of excess FE to prevent hydrolysis reactions. The kinetics are consistent with a direct IES reaction of **10** with dihydrogen, similar, albeit slower, to that observed for the monomeric hydroxide **1**.

It is evident from this study that hydrogenolysis of Pd−OR bonds can occur in a directly analogous fashion to the Pd−OH reaction with the caveat that inhibition by dimer formation is not generally observed for the alkoxides. In addition, in the case of the production of acidic alcohols, hydrogenolysis is thermodynamically unfavorable. Finally, there are significant competing side reactions evident for alkoxide complexes. DBHA generates the same palladium product as hydrogenolysis, but instead of the alchohol, unsaturated organics are produced. DBHA can be promoted with the addition of the alcohol, and it can be minimized through the use of sterically bulky alkoxides or with electron-withdrawing substituents on the alkoxide. Finally, hydrolysis followed by hydrogenolysis of the Pd−OH will actually generate the identical products as hydrogenolysis of the Pd−OR complex. Thus, hydrogenolysis of metal hydroxides and metal alkoxides can both lead to regeneration of a metal hydride in a catalytic cycle. The wide range of substrates Pd−OR (R = H, CH_3, C_6H_5, $CH_2C(CH_3)_3$, CH_2CF_3, CH_2CHF_2, CH_2CH_2F) examined in this study helps to clarify the conditions and the considerations necessary for the successful utilization of this hydrogenolysis reaction in a catalytic system.

EXPERIMENTAL SECTION

Unless specified otherwise, all manipulations were carried out under nitrogen using conventional vacuum line techniques or a glovebox equipped with a −35 °C freezer. Solvents were purified before use. THF, benzene, and pentane were purified by passage through columns of activated alumina and molecular sieves. C_6D_6 was dried over sodium metal/benzophenone. Fluoroethanols were dried over activated molecular sieves (3 Å) and distilled under a nitrogen atmosphere. Unless otherwise noted, all other reagents were used as obtained from commercial suppliers. NMR spectra were obtained at room temperature (25 °C) on Bruker AV300 and AV500 MHz spectrometers, with chemical shifts (δ) reported in ppm. All ^{1}H NMR spectra were referenced to the residual protiated solvent signal; ^{31}P NMR and ^{19}F NMR spectra were referenced externally to 85% H_3PO_4 (0 ppm) and CF_3COOH (−76.55 ppm), respectively. All ^{13}C and ^{31}P NMR data were collected proton-decoupled ($^{13}C\{^1H\}$ and $^{31}P\{^1H\}$). All ^{1}H and ^{13}C resonances were assigned using gradient-selected heteronuclear multiple-quantum coherence (gsHMQC) NMR spectroscopy and gradient-selected correlation spectroscopy (gsCOSY). Multiplicity is reported as follows: s, singlet; d, doublet; t, triplet; q, quartet; vt, virtual triplet; br, broad. Figure 14 illustrates the aromatic carbon-numbering scheme for all reported NMR data. Elemental analyses were carried out by Atlantic Microlab, Inc. of Norcross, GA. All crystallographic data was collected at the University of Washington X-ray crystallography lab. H_2-pressurized NMR-scale reactions were achieved using a gas pressurization apparatus.[45] The following complexes were prepared according to

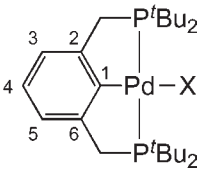

Figure 14. Aromatic carbon-numbering scheme for (^{tBu}PCP)Pd complexes.

published procedures: ($^{t\text{Bu}}$PCP)PdOH (**1**),[18] ($^{t\text{Bu}}$PCP)PdH (**2**),[18] ($^{t\text{Bu}}$PCP)PdOCH$_3$ (**3**),[9] ($^{t\text{Bu}}$PCP)PdONO$_2$.[20]

Safety Note: Great caution must be taken when handling and heating pressurized medium-walled NMR tubes. At all times, pressurized NMR tubes were heated inside stainless steel jackets and transported and stored in a protective plastic jacket.

Kinetic Studies: Reaction of 1 and H_2. In a typical experiment, a C_6D_6 solution of **1** (4.2 mM), H_2O (37.8 mM), and hexamethylbenzene (internal standard) was transferred to a medium-walled NMR tube fitted with a resealable Telflon valve. The sample was degassed by three freeze−pump−thaw cycles and then placed under hydrogen pressure (7.0 or 3.5 atm) using a gas pressurization apparatus.[45] Samples were placed in a 25 °C temperature-controlled oil bath during the reaction. Rates were determined by following the disappearance of the methylene signal (CH_2P) of **1** through three half-lives, as compared to the methyl signal of hexamethylbenzene.

Reaction of 3 with H_2. Formation of ($^{t\text{Bu}}$PCP)PdH (2). A medium-walled NMR tube fitted with a resealable Teflon valve was charged with complex **3** (2.0 mg, 3.9 μmol) and hexamethylbenzene (internal standard). The solids were then dissolved in C_6D_6 (0.4 mL). The solution was degassed, and the desired hydrogen pressure was added. The reaction was monitored by ^{1}H NMR spectroscopy, and the disappearance of **3**, along with the appearance of **2** and methanol, was observed.

Reaction of 3 with (*p*-OCH$_2$)$_n$. Formation of ($^{t\text{Bu}}$PCP)PdOCH$_2$OCH$_3$ (4). An NMR tube fitted with a resealable Teflon valve was charged with complex **3** (2.2 mg, 4.1 μmol), *para*-formaldehyde (1.2 mg, 40 μmol), and the internal standard hexamethylbenzene (1.0 mg, 6.2 μmol). Benzene-d_6 (0.4 mL) was vacuum transferred into the tube, and the solution was immediately analyzed by NMR spectroscopy. The partial conversion of **3** and formation of ($^{t\text{Bu}}$PCP)PdOCH$_2$OCH$_3$ (**4**) was observed: ^{1}H NMR (C_6D_6, 500 MHz) δ = 7.01 (t, 1H, J_{HH} = 7.3 Hz, ***H***4), 6.92 (d, 2H, J_{HH} = 7.3 Hz, ***H***3,5), 5.72 (s, 2H, OC***H***$_2$OCH$_3$), 3.65 (s, 3H, OCH$_2$OC***H***$_3$), 2.93 (vt, 4H, J_{HP} = 3.4 Hz, C***H***$_2$P), 1.29 (vt, 36H, J_{HP} = 6.5 Hz, C(C***H***$_3$)$_3$). ^{31}P{^{1}H} NMR (C_6D_6, 203 MHz) δ = 70.9. After an additional 30 min, the complete conversion of **3** had occurred. In the ^{1}H NMR spectrum, complex **4** was observed along with numerous peaks between 3−4 ppm and 4.5−6 ppm, corresponding to −OC***H***$_2$− and −OC***H***$_3$ protons of ($^{t\text{Bu}}$PCP)Pd(OCH$_2$)$_n$OCH$_3$ complexes, respectively, resulting from an additional *n* number of insertions of OCH$_2$ into the Pd−O bond of **3**. In the ^{31}P{^{1}H} NMR spectrum, several overlapping singlets resonated at 72−70 ppm.

Reaction of 3 with H_2O. A standard solution of complex **3** (25 mM) and the internal standard hexamethylbenzene (13 mM) was made in benzene-d_6. Performed in triplicate, 0.380 mL of the stock solution of complex **3** (5.0 mg, 9.4 μmol) was transferred by syringe into an NMR tube with a resealable Teflon valve. After initial ^{1}H and ^{31}P{^{1}H} NMR spectra were acquired, each NMR tube was treated with nearly 0.5 equiv of water (120 μL of a 33 mM H_2O solution in C_6D_6, 4.0 μmol).[46] The total volume of the solution was 0.500 mL, [**3**]$_0$ = 19 mM, and [H_2O]$_0$ = 8.0 mM. The partial conversion of complex **3** and water to **1** and methanol was observed by NMR spectroscopy. The concentrations of **1**, **3**, methanol, and water[33] were measured by integration against the methyl signal of hexamethylbenzene over the course of 5 h until concentrations equilibrated.

Reaction of 1 with CH_3OH. A benzene-d_6 solution (0.400 mL) of complex **1** (26.5 mM) and hexamethylbenzene (13 mM) was added to an NMR tube with a resealable Teflon valve. Initial ^{1}H and ^{31}P{^{1}H} NMR spectra were collected. The solution was then treated with 1 equiv of methanol (0.43 μL, 10.6 μmol), and the reaction mixture was monitored by ^{1}H NMR spectroscopy. Over the course of 2 days, only a small amount of complex **1** (<10%) had converted to complex **3**.

($^{t\text{Bu}}$PCP)PdOC$_6$H$_5$ (5). The nitrato complex ($^{t\text{Bu}}$PCP)PdONO$_2$ (75.5 mg, 0.134 mmol) was added to a round-bottom flask along with an excess of KOC$_6$H$_5$ (26.0 mg, 0.197 mmol). The solids were dissolved in THF (15 mL), and the light orangish-yellow colored solution was stirred for 4 h. The volatiles were removed under reduced pressure, and the peach-colored solid was extracted with benzene (20 mL) and filtered through a Teflon filter (0.2 μm). The solvent was removed from the filtrate under vacuum, leaving a peach solid which was then dissolved in a minimum of benzene (0.5 mL). The solution was layered with pentane (4 mL) and cooled to −35 °C for 3 days. During this time, faint-yellow crystals formed. The solvent was decanted, and the crystals were dried in vacuo. Yield: 38.2 mg (48.1%). ^{1}H NMR (C_6D_6, 500 MHz) δ = 7.38 (t, 2H, $^3J_{HH}$ = 7.1 Hz, *m*-Ph-***H***), 7.08 (d, 2H, $^3J_{HH}$ = 7.5 Hz, *o*-Ph-***H***), 7.03 (t, 1H, $^3J_{HH}$ = 7.5 Hz, ***H***4), 6.92 (d, 2H, $^3J_{HH}$ = 7.5 Hz, ***H***3,5), 6.73 (t, 2H, $^3J_{HH}$ = 7.5 Hz, *p*-Ph-***H***), 2.94 (vt, 4H, $^2J_{HP}$ = 3.7 Hz, C***H***$_2$P), 1.21 (vt, 36H, $^3J_{HP}$ = 6.8 Hz, C(C***H***$_3$)$_3$). ^{13}C{^{1}H} NMR (C_6D_6, 126 MHz) δ = 171.3 (s, *i*-Ph-***C***), 155.7 (s, ***C***1), 151.7 (vt, $^3J_{CP}$ = 10.3 Hz, ***C***2,6), 129.1 (s, *m*-Ph-***C***), 125.0 (s, ***C***4), 122.5 (vt, $^3J_{CP}$ = 10.0 Hz, ***C***3,5), 121.1 (s, *o*-Ph-***C***), 112.1 (s, *p*-Ph-***C***), 34.7 (vt, $^1J_{CP}$ = 7.0 Hz, ***C***(CH$_3$)$_3$), 34.1 (vt, $^1J_{CP}$ = 10.2 Hz, ***C***H$_2$P), 29.4 (s br, C(***C***H$_3$)$_3$). ^{31}P{^{1}H} NMR (C_6D_6, 203 MHz) δ = 70.90. Anal. Calcd for $C_{30}H_{48}OP_2Pd$: C, 60.76; H, 8.16. Found: C, 60.82; H, 8.20.

Reaction of 2 with HOPh. Formation of [(μ-$^{t\text{Bu}}$PCHP)Pd]$_2$ (6). Complex **2** (6.0 mg, 12 μmol), phenol (2.3 mg, 24 μmol), and hexamethylbenzene (1−2 flakes, internal standard) were weighed into a medium-walled NMR tube fitted with a resealable Teflon valve. C_6D_6 (0.4 mL) was vacuum transferred into the tube, and once the solids dissolved, immediate formation of bubbles was observed. ^{1}H NMR spectroscopy revealed the initial formation of the phenoxide complex **5** and free H_2, and over the course of 2 h, the solution changed from colorless to pale-yellow. The formation of faint-yellow crystals occurred over a period of 2 days, which were identified by X-ray crystallography as [(μ-$^{t\text{Bu}}$PCHP)Pd]$_2$ (**6**).

($^{t\text{Bu}}$PCP)PdOCH$_2$C(CH$_3$)$_3$ (7). The nitrato complex ($^{t\text{Bu}}$PCP)PdONO$_2$ (171.3 mg, 0.305 mmol) was added to a round-bottom flask along with an excess of KOCH$_2$C(CH$_3$)$_3$ (58.7 mg, 0.465 mmol). The solids were dissolved in THF (20 mL), and the pale orange-colored solution was stirred for 12 h. The volatiles were removed under reduced pressure, and the peach-colored solid was extracted with benzene (25 mL) and filtered through a Teflon filter. The solvent was removed from the filtrate under vacuum, leaving a peach-colored solid. Complex **7** was redissolved in pentane and was recrystallized from a slow evaporation of the solution. Yield: 88.7 mg (49.6%). ^{1}H NMR (C_6D_6, 500 MHz) δ = 7.04 (t, 1H, $^3J_{HH}$ = 7.4 Hz, ***H***4), 6.96 (d, 2H, $^3J_{HH}$ = 7.4 Hz, ***H***3,5), 4.06 (s, 2H, OC***H***$_2$C(CH$_3$)$_3$), 2.98 (vt, 4H, $^2J_{HP}$ = 3.8 Hz, C***H***$_2$P), 1.31 (vt, 36H, $^3J_{HP}$ = 6.6 Hz, C(C***H***$_3$)$_3$), 1.31 (s, 9H, OCH$_2$C(C***H***$_3$)$_3$). ^{13}C{^{1}H} NMR (C_6D_6, 126 MHz) δ = 158.4 (s, ***C***1), 151.3 (vt, $^2J_{CP}$ = 10.0 Hz, ***C***2,6), 124.5 (s, ***C***4), 121.9 (vt, $^3J_{CP}$ = 9.6 Hz, ***C***3,5), 85.9 (s, O***C***H$_2$C(CH$_3$)$_3$), 36.6 (OCH$_2$***C***(CH$_3$)$_3$), 35.2 (vt, $^1J_{CP}$ = 10.2 Hz, ***C***H$_2$P), 34.8 (vt, $^1J_{CP}$ = 6.7 Hz, ***C***(CH$_3$)$_3$), 29.4 (vt, $^2J_{CP}$ = 3.3 Hz, C(***C***H$_3$)$_3$), 28.4 (s, OCH$_2$C(***C***H$_3$)$_3$). ^{31}P{^{1}H} NMR (C_6D_6, 203 MHz) δ = 68.87. Anal. Calcd for $C_{29}H_{54}OP_2Pd$: C, 59.33; H, 9.27. Found: C, 59.28; H, 9.33.

Reaction of 2 with HOCH$_2$CF$_3$. Formation of ($^{t\text{Bu}}$PCP)PdOCH$_2$CF$_3$ (8). Complex **2** (3.0 mg, 6.0 μmol) was weighed into a medium-walled NMR tube fitted with a resealable Teflon valve. The complex was dissolved in C_6D_6 (0.40 mL). An excess of deoxygenated 2,2,2-trifluoroethanol (5.0 μL, 70 μmol) was added by syringe. Immediate formation of bubbles was observed, and upon closer inspection by NMR spectroscopy, complete conversion of **2** to the 2,2,2-trifluoroethoxide complex **8** and H_2 had occurred. ^{1}H NMR (C_6D_6, 500 MHz) δ = 7.00 (t, 1H, $^3J_{HH}$ = 7.3 Hz, ***H***4), 6.89 (d, 1H, $^3J_{HH}$ = 7.3 Hz, ***H***3,5), 4.65 (q, 2H, $^3J_{HF}$ = 9.9 Hz, C***H***$_2$CF$_3$), 2.89 (vt, 4H, $^2J_{HP}$ = 3.8 Hz, C***H***$_2$P), 1.23 (vt, 36H, $^3J_{HP}$ = 6.7 Hz, C(C***H***$_3$)$_3$). ^{13}C{^{1}H} NMR (C_6D_6, 126 MHz) δ = 156.3 (s, ***C***1), 151.5 (vt, $^2J_{CP}$ = 10.2 Hz, ***C***2,6), 124.8 (***C***4), 122.2 (vt, $^3J_{CP}$ = 9.9 Hz, ***C***3,5), 128.5 (q, $^1J_{CF}$ = 284.2 Hz, CH$_2$***C***F$_3$), 72.0 (q, $^2J_{CF}$ = 29.6 Hz, ***C***H$_2$CF$_3$), 34.7 (vt, $^1J_{CP}$ = 7.0 Hz, ***C***(CH$_3$)$_3$), 34.4 (vt, $^1J_{CP}$ = 10.2 Hz, ***C***H$_2$P), 29.2 (vt, $^2J_{CP}$ = 3.2 Hz, C(***C***H$_3$)$_3$). ^{31}P{^{1}H} NMR (C_6D_6, 203 MHz) δ = 70.91. ^{19}F NMR (C_6D_6, 282 MHz) δ = −73.3 (t, $^3J_{FH}$ = 9.9 Hz).

Reaction of 2 with $HOCH_2CHF_2$. Formation of (^{tBu}PCP)Pd-OCH_2CHF_2 (9). Complex **2** (3.0 mg, 6.0 μmol) was weighed into a medium-walled NMR tube fitted with a resealable Teflon valve. The complex was dissolved in C_6D_6 (0.40 mL). An excess of deoxygenated 2,2-difluoroethanol (5.0 μL, 79 μmol) was added by syringe. The complete conversion of complex **2** to the 2,2-difluoroethoxide complex **9** and H_2 was observed by NMR spectroscopy over the course of 4 h. ^{1}H NMR (C_6D_6, 500 MHz) δ = 7.01 (t, 1H, $^3J_{HH}$ = 7.2 Hz, ***H***4), 6.91 (d, 1H, $^3J_{HH}$ = 7.2 Hz, ***H***3,5), 6.07 (tt, 1H, $^2J_{HF}$ = 58.0 Hz, C***H***F_2, $^3J_{HH}$ = 4.2 Hz) 4.51 (td, 2H, $^3J_{HF}$ = 15.2 Hz, $^3J_{HH}$ = 4.2 Hz, CH_2CHF_2), 2.91 (vt, 4H, $^2J_{HP}$ = 3.8 Hz, CH_2P), 1.24 (vt, 36H, $^3J_{HP}$ = 6.7 Hz, C(CH_3)$_3$). ^{13}C{^{1}H} NMR (C_6D_6, 126 MHz) δ = 156.3 (s, ***C***1), 151.4 (vt, $^2J_{CP}$ = 10.0 Hz, ***C***2,6), 124.9 (***C***4), 122.2 (vt, $^3J_{CP}$ = 9.8 Hz, ***C***3,5), 120.3 (t, $^1J_{CF}$ = 244.1 Hz, CH_2***C***HF_2), 73.7 (t, $^2J_{CF}$ = 24.1 Hz, ***C***H_2CHF_2), 34.8 (vt, $^1J_{CP}$ = 6.7 Hz, ***C***(CH$_3$)$_3$), 34.4 (vt, $^1J_{CP}$ = 10.3 Hz, ***C***H_2P), 29.3 (vt, $^2J_{CP}$ = 3.2 Hz, C(***C***H$_3$)$_3$). ^{31}P{^{1}H} NMR (C_6D_6, 203 MHz) δ = 70.42. ^{19}F NMR (C_6D_6, 282 MHz) δ = −124.5 (dt, $^2J_{FH}$ = 58.0 Hz, $^3J_{FH}$ = 15.2 Hz).

(^{tBu}PCP)PdOCH_2CH_2F (10). Complex **7** (256.0 mg, 436 μmol) was added to a modified H-flask[47] fitted with a resealable Teflon valve and dissolved in benzene (5 mL). To the solution, an excess of 2-fluoroethanol (50 μL, 850 μmol) was added by syringe. The reaction was stirred for 2 h, whereupon the volatiles were removed under vacuum. The resulting brown solid was dried under reduced pressure using a vacuum line. Benzene (5 mL) was vacuum transferred into the H-flask to dissolve the solids. With the solution under static vacuum, a cold bath (evaporating acetone, 19 °C) was used to slowly vacuum transfer the benzene from one well of the H-flask to the other. Over the course of two days, tan-colored crystals of **10** formed as the solution gradually concentrated. The supernatant was decanted, and the crystals of **10** were isolated and pumped to dryness on the vacuum line. Yield: 138.7 mg (56.5%). ^{1}H NMR (C_6D_6, 500 MHz) δ = 7.03 (t, 1H, $^3J_{HH}$ = 7.4 Hz, ***H***4), 6.93 (d, 1H, $^3J_{HH}$ = 7.4 Hz, ***H***3,5), 4.78 (dt, 2H, $^2J_{HF}$ = 48.7 Hz, $^3J_{HH}$ = 5.7 Hz, CH_2F), 4.53 (dt, 2H, $^3J_{HF}$ = 21.3 Hz, $^3J_{HH}$ = 5.7 Hz, CH_2CH$_2$F), 2.94 (vt, 4H, $^2J_{HP}$ = 3.6 Hz, CH_2P), 1.28 (vt, 36H, $^3J_{HP}$ = 6.7 Hz, C(CH_3)$_3$). ^{13}C{^{1}H} NMR (C_6D_6, 126 MHz) δ = 157.9 (s, ***C***1), 151.5 (vt, $^2J_{CP}$ = 10.1 Hz, ***C***2,6), 124.6 (***C***4), 122.0 (vt, $^3J_{CP}$ = 9.8 Hz, ***C***3,5), 88.9 (d, $^1J_{CF}$ = 171.0 Hz, CH_2***C***H_2F), 72.1 (t, $^2J_{CF}$ = 20.2 Hz, ***C***H_2CH$_2$F), 32.7 (vt, $^1J_{CP}$ = 10.1 Hz, ***C***H_2P), 32.7 (vt, $^1J_{CP}$ = 6.8 Hz, ***C***(CH$_3$)$_3$), 29.3 (vt, $^2J_{CP}$ = 3.4 Hz, C(***C***H$_3$)$_3$). ^{31}P{^{1}H} NMR (C_6D_6, 203 MHz) δ = 69.86. ^{19}F NMR (C_6D_6, 282 MHz) δ = −218.6 (tt, $^2J_{FH}$ = 48.7 Hz, $^3J_{FH}$ = 21.3 Hz). Anal. Calcd for $C_{26}H_{47}FOP_2Pd$: C, 55.47; H, 8.41. Found: C, 55.35; H, 8.64.

Control Experiment: Complex 10 in C_6D_6 with Excess FE in Absence of H_2. Complex **10** (2.0 mg, 3.6 μmol), 2-fluoroethanol (1.9 μL, 32 μmol), and hexamethylbenzene (1−2 flakes, internal standard) were added to a medium-walled NMR tube fitted with a resealable Teflon valve. The NMR tube was sealed under an atmosphere of N_2 and heated to 60 °C in a temperature-controlled oil bath. The sample was analyzed by ^{1}H NMR spectroscopy over the course of 7 days, during which <5% conversion of **10** to **2** was observed.

Kinetic Studies: Reaction of 10 and H_2. In a typical experiment, a medium-walled NMR tube fitted with a resealable Teflon valve was charged with complex **10** (2.0 mg, 3.6 μmol), 2-fluoroethanol (1.9 μL, 32 μmol), and hexamethylbenzene (1−2 flakes, internal standard). Using a vacuum line, 0.40 mL of the C_6D_6 was vacuum transferred from a sodium−potassium alloy into the NMR tube. The degassed sample was then placed under hydrogen pressure (7.0−3.5 atm) using a gas pressurization apparatus.[45] Initial ^{1}H NMR spectra were collected before heating the sample to 60 °C in a temperature-controlled oil bath. Rates were determined by following the disappearance of complex **10**'s −CH_2F resonance through three half-lives, as compared to the methyl signal of hexamethylbenzene.

Fluoroethanol NMR Spectroscopic Data. 2,2,2-Trifluoroethanol: ^{1}H NMR (C_6D_6, 500 MHz) δ = 3.41 (q, 2H, $^3J_{HF}$ = 8.8 Hz, CH_2CF$_3$), 3.29 (s, 1H, O***H***). ^{19}F NMR (C_6D_6, 282 MHz) δ = −76.54 (t, $^3J_{FH}$ = 8.9 Hz). 2,2-Difluoroethanol: ^{1}H NMR (C_6D_6, 500 MHz) δ = 5.26 (tt, 1H, $^2J_{HF}$ = 55.8 Hz, $^3J_{HH}$ = 3.8 Hz, C***H***F_2), 3.18 (td, 2H, $^3J_{HH}$ = 3.8 Hz, $^3J_{HF}$ = 14.7 Hz, CH_2CHF_2), 2.04 (s, 1H, O***H***). ^{19}F NMR (C_6D_6, 282 MHz) δ = −126.2 (dt, $^2J_{FH}$ = 55.8 Hz, $^3J_{FH}$ = 14.7 Hz). 2-Fluoroethanol: ^{1}H NMR (C_6D_6, 500 MHz) δ = 4.21 (dt, 2H, $^2J_{HF}$ = 48.0 Hz, $^3J_{HH}$ = 4.2 Hz, CH_2F), 4.00 (s, 1H, O***H***), 3.51 (dt, 2H, $^3J_{HF}$ = 29.8 Hz, $^3J_{HH}$ = 4.2 Hz, CH_2CH$_2$F). ^{19}F NMR (C_6D_6, 282 MHz) δ = −224.4 (tt, $^2J_{FH}$ = 48.0 Hz, $^3J_{FH}$ = 29.8 Hz).[48]

■ ASSOCIATED CONTENT

Supporting Information. X-ray crystallographic data including files in CIF format for **1**•**FE**, **5**, **6**, **7**, and **10**, as well as additional kinetic plots, computational methodology and XYZ coordinates, and apparatus diagrams. This material is available free of charge via the Internet at http://pubs.acs.org.

■ AUTHOR INFORMATION

Corresponding Author
goldberg@chem.washington.edu; rakemp@unm.edu

■ ACKNOWLEDGMENT

We thank Richard P. Muller for computations, Alexander J. M. Miller for insightful discussions, and the Department of Energy (DE-FG02-06ER15765) for support.

■ REFERENCES

(1) Hartwig, J. F. *Organotransition Metal Chemistry: From Bonding to Catalysis*; University Science Books: Sausalito, CA, 2010.
(2) Crabtree, R. H. *The Organometallic Chemistry of the Transition Metals*, 4th ed.; John Wiley & Sons: New York, 2005.
(3) *Handbook of Homogeneous Hydrogenation*; De Vries, J. G., Elsevier, C. J., Eds.; Wiley-VCH: Weinheim, Germany, 2007.
(4) Esteruelas, M. A.; Oro, L. A. *Chem. Rev.* **1998**, *98*, 577.
(5) (a) Maron, L.; Eisenstein, O. *J. Am. Chem. Soc.* **2001**, *123*, 1036. (b) Lee, J. C., Jr.; Peris, E.; Rheingold, A. L.; Crabtree, R. H. *J. Am. Chem. Soc.* **1994**, *116*, 11014. (c) Joshi, A. M.; James, B. R. *Organometallics* **1990**, *9*, 199. (d) Watson, P. L.; Parshall, G. W. *Acc. Chem. Res.* **1985**, *18*, 51.
(6) (a) Samec, J. S. M.; Bäckvall, J. E.; Andersson, P. G.; Brandt, P. *Chem. Soc. Rev.* **2006**, *35*, 237. (b) Noyori, R.; Ohkuma, T. *Angew. Chem., Int. Ed.* **2001**, *40*, 40.
(7) (a) Conley, B. L.; Pennington-Boggio, M. K.; Boz, E.; Williams, T. J. *Chem. Rev.* **2010**, *110*, 2294. (b) Blum, Y.; Czarkie, D.; Rahamim, Y.; Shvo, Y. *Organometallics* **1985**, *4*, 1459.
(8) This type of intramolecular proton transfer has been termed internal electrophilic substitution (IES). (a) Oxgaard, J.; Tenn, W. J., III; Nielsen, R. J.; Periana, R. A.; Goddard, W. A., III. *Organometallics* **2007**, *26*, 1565. (b) Cundari, T. R.; Grimes, T. V.; Gunnoe, T. B. *J. Am. Chem. Soc.* **2007**, *129*, 13172.
(9) For a preliminary report on the hydrogenolysis of palladium(II) hydroxide and methoxide pincer complexes, see: Fulmer, G. R.; Muller, R. P.; Kemp, R. A.; Goldberg, K. I. *J. Am. Chem. Soc.* **2009**, *131*, 1346.
(10) Bryndza, H. E.; Fong, L. K.; Paciello, R. A.; Tam, W.; Bercaw, J. E. *J. Am. Chem. Soc.* **1987**, *109*, 1444.
(11) (a) Blum, O.; Milstein, D. *J. Organomet. Chem.* **2000**, *479*, 593. (b) Ritter, J. C. M.; Bergman, R. G. *J. Am. Chem. Soc.* **1998**, *120*, 6826. (c) Blum, O.; Milstein, D. *J. Am. Chem. Soc.* **1995**, *117*, 4582.
(12) Pearlman, W. M. *Tetrahedron Lett.* **1967**, 1663.
(13) (a) Adams, R.; Shriner, R. L. *J. Am. Chem. Soc.* **1923**, *45*, 2171. (b) Carothers, W. H.; Adams, R. *J. Am. Chem. Soc.* **1923**, *45*, 1071. (c) Voorhees, V.; Adams, R. *J. Am. Chem. Soc.* **1922**, *44*, 1397.

(14) (a) Deutsch, C.; Krause, N.; Lipshutz, B. H. *Chem. Rev.* **2008**, *108*, 2916. (b) Mahoney, W. S.; Brestensky, D. M.; Stryker, J. M. *J. Am. Chem. Soc.* **1988**, *110*, 291. (c) Goeden, G. V.; Caulton, K. G. *J. Am. Chem. Soc.* **1981**, *103*, 7354.
(15) Jessop, P. G.; Ikariya, T.; Noyori, R. *Chem. Rev.* **1995**, *95*, 259.
(16) Wenzel, T. T. *Dioxygen Activation and Homogeneous Catalytic Oxidation*; Simándi, L. I., Ed.; Studies in Surface Science and Catalysis 66; Elsevier Science Publishers B. V.: Amsterdam, 1991; p 545.
(17) (a) Joanna, R.; Webb, J. R.; Munro-Leighton, C.; Pierpont, A. W.; Gurkin, J. T.; Gunnoe, T. B.; Cundari, T. R.; Sabat, M.; Petersen, J. L.; Boyle, P. D. *Inorg. Chem.* **2011**, *50*, 4195. (b) Webb, J. R.; Pierpont, A. W.; Colleen Munro-Leighton, C.; T. Brent Gunnoe, T. B.; Cundari, T. R.; Boyle, P. D. *J. Am. Chem. Soc.* **2010**, *132*, 4520. (c) Böhler, C.; Avarvari, N.; Schönberg, H.; Wörle, M.; Rüegger, H.; Grützmacher, H. *Helv. Chim. Acta* **2001**, *84*, 3127. (d) Thompson, J. S.; Randall, S. L.; Atwood, J. D. *Organometallics* **1991**, *10*, 3906. (e) Thompson, J. S.; Bernard, K. A.; Rappoli, B. J.; Atwood, J. D. *Organometallics* **1990**, *9*, 2727.
(18) Denney, M. C.; Smythe, N. A.; Cetto, K. L.; Kemp, R. A.; Goldberg, K. I. *J. Am. Chem. Soc.* **2006**, *128*, 2508.
(19) Fulmer, G. R.; Miller, A. J. M.; Sherden, N. H.; Gottlieb, H. E.; Nudelman, A.; Stoltz, B. M.; Bercaw, J. E.; Goldberg, K. I. *Organometallics* **2010**, *29*, 2176.
(20) Johansson, R.; Öhrström, L.; Wendt, O. F. *Cryst. Growth Des.* **2007**, *7*, 1974.
(21) 9 equiv corresponds to a water concentration of 38 mM, very close to the reported solubility of water in benzene at 25 °C (36 mM). Karlsson, R. *J. Chem. Eng. Data* **1973**, *18*, 290.
(22) Derived from an Ostwald coefficient of 0.0718, hydrogen concentrations were calculated to be 21 mM (8.2 μmol) and 10 mM (4.1 μmol) for 7.0 and 3.5 atm, respectively. Young, C. L. *Hydrogen and Deuterium, Solubility Data Series*; Pergamon Press: Oxford, 1981; Vol. 5/6.
(23) Espenson, J. H. *Chemical Kinetics and Reaction Mechanisms*, 2nd ed.; McGraw-Hill: New York, 1995; p 82.
(24) Cámpora, J.; Palma, P.; del Río, D.; Álvarez, E. *Organometallics* **2004**, *23*, 1652.
(25) Billo, E. J. *Excel for Chemists*, 2nd ed.; John Wiley & Sons, Inc.: Canada, 2001; p 184.
(26) Additional data concerning the Rugga−Kutta Fourth Order method can be found in the Supporting Information.
(27) (a) Hull, K. L.; Lanni, E. L.; Sanford, M. S. *J. Am. Chem. Soc.* **2006**, *128*, 14047. (b) Canty, A. *Acc. Chem. Res.* **1992**, *25*, 83.
(28) (a) Milet, A.; Dedieu, A.; Kapteijn, G. M.; van Koten, G. *Inorg. Chem.* **1997**, *36*, 3223. (b) Hutschka, F.; Dedieu, A.; Eichberger, M.; Fornika, R.; Leitner, W. *J. Am. Chem. Soc.* **1997**, *119*, 4432. (c) Hutschka, F.; Dedieu, A.; Leitner, W. *Angew. Chem., Int. Ed. Engl.* **1995**, *34*, 1742.
(29) (a) Cundari, T. R.; Grimes, T. V.; Gunnoe, T. B. *J. Am. Chem. Soc.* **2007**, *129*, 13172. (b) Oxgaard, J.; Tenn, W. J., III; Nielsen, R. J.; Periana, R. A.; Goddard, W. A., III. *Organometallics* **2007**, *26*, 1565.
(30) Kimmich, B. F. M.; Bullock, R. M. *Organometallics* **2002**, *21*, 1504.
(31) (a) Pawlikowski, A. V.; Getty, A. D.; Goldberg, K. I. *J. Am. Chem. Soc.* **2007**, *129*, 10382. (b) Williams, B. S.; Goldberg, K. I. *J. Am. Chem. Soc.* **2001**, *123*, 2576.
(32) See the Supporting Information for computational methodology, XYZ coordinates, and additional energy data.
(33) Integrations of the ^{1}H NMR resonance for water were not accurate due to exchange with the hydroxide complex **1**; therefore, the concentration of water was determined by subtracting [CH_3OH] from the initial concentration of water ([H_2O]$_0$).
(34) Bryndza, H. E.; Tam, W. *Chem. Rev.* **1988**, *88*, 1163.
(35) Smythe, N. A.; Grice, K. A.; Williams, B. S.; Goldberg, K. I. *Organometallics* **2009**, *28*, 277.
(36) Fafard, C. M.; Ozerov, O. V. *Inorg. Chim. Acta* **2007**, *360*, 286.
(37) Melero, C.; Martínez-Prieto, L. M.; Plama, P.; del Rio, D.; Álvarez, E.; Cámpora, J. *Chem. Commun.* **2010**, *46*, 8851.
(38) Bruice, P. Y. *Organic Chemistry*, 3rd ed.; Prentice Hall: NJ, 2001; p 645.
(39) For space-filling diagrams of **1**, **3**, **5**, **7**, and **10**, see Figure S6 in the Supporting Information.
(40) Smith, M. B.; March, J. *March's Advanced Organic Chemistry: Reactions, Mechanisms, and Structure*, 5th ed.; John Wiley & Sons: New York, 2001; p 1176.
(41) Ballinger, P.; Long, F. A. *J. Am. Chem. Soc.* **1960**, *82*, 795.
(42) Mock, W. L.; Zhang, J. Z. *Tetrahedron Lett.* **1990**, 5687.
(43) For additional kinetic plots, see Figure S1 in the Supporting Information.
(44) It was considered that the hydrogenolysis of **10** could proceed exclusively via path **b** (Scheme 5) in the presence of excess FE but follows a well-behaved first-order dependency on Pd if [H_2O] were too low for **1** to dimerize. However, when hydrogenolysis reactions were performed on **1** in the presence of a drying agent ($MgSO_4$), the reaction kinetics were still observed to be half-order in [**1**], indicating that dimerization still occurs when H_2O concentrations are below the detection limit of ^{1}H NMR spectroscopy.
(45) For diagrams of gas pressurization apparatus, see Figures S2−S3 in the Supporting Information.
(46) Notably, the reported solubility of water in benzene at 25 °C is 36 mM. See ref 21.
(47) For a diagram of modified H-flask, see Figure S4 in the Supporting Information.
(48) For more information on fluoroethanols, see: Elliott, A. J. *Fluoroethanols: Kirk-Othmer Encyclopedia of Chemical Terminology*; John Wiley & Sons: 2000.